Characterization of Anaerobic Growth and Biofilm formation in *Pseudomonas aeruginosa* mutant strain lacking genes PA1759 and PA1760

Heloisa Burian

A Thesis Submitted to the University of Ottawa in Partial Fulfillment of the Requirements for the Master's of Science degree in Microbiology and Immunology

Department of Biochemistry, Microbiology, and Immunology

Faculty of Medicine

University of Ottawa

Abstract

Antibiotic resistance is a major problem in the 21st century. Opportunistic bacterial infections caused by *Pseudomonas aeruginosa* (PA) impact individuals with compromised immune systems, like those with cystic fibrosis (CF). Due to PA's capacity to become resistant to antibiotics through many mechanisms, including the formation of biofilms, this is a pathogen to be concerned about. PA's antibiotic resistance mechanisms built into the organism's genome play a role in this resistance.

Prior research involved screening a sub-library of transposon-insertion mutants (tn-mutants) to identify transcriptional regulators (TRs) deemed important to biofilm antibiotic resistance. Thirteen such TRs were identified, and these were thought to be potentially relevant in intrinsic antibiotic resistance. Among these TRs, the tn-mutant PA1759 stood out due to having the strongest biofilm antibiotic susceptibility phenotype. PA1759 is found in an operon with PA1760, so a Δ*PA1759-60* double deletion mutant was constructed and analyzed. Compared to the wild-type (WT) biofilm, the Δ*PA1759-60* mutant is four times more susceptible to Tobramycin (Tb) when its biofilm is exposed to antibiotics. This suggested that *PA1759-60* is an important regulator of antibiotic resistance, necessitating further research into its processes and potential as a therapeutic target.

This research aimed to analyze the Δ*PA1759-60* mutant to determine its growth and biofilm formation potential under aerobic as well as anaerobic conditions compared to the WT. Given that PA often resides in anaerobic environments, such as within the CF lung, characterization under the two conditions is important in assessing potential clinical outcome. The Δ*PA1759-60* mutant had much reduced growth and biofilm formation compared to the WT under anaerobic conditions, consistent with prior observations under aerobic conditions. These

findings emphasize the reduced biofilm formation of Δ*PA1759-60*, providing useful insights for future development of targeted therapies for PA infections in anaerobic conditions.

Résumé

La résistance aux antibiotiques est un problème majeur au 21e siècle. Les infections bactériennes opportunistes causées par *Pseudomonas aeruginosa* (PA) affectent les individus dont le système immunitaire est affaibli, comme ceux atteints de fibrose kystique (FK). En raison de la capacité de PA à devenir résistante aux antibiotiques par divers mécanismes, y compris la formation de biofilms, ce pathogène représente une menace sérieuse. Les mécanismes de résistance aux antibiotiques de PA intégrés dans le génome de l'organisme jouent un rôle crucial dans cette résistance.

Des recherches antérieures ont impliqué le criblage d'une sous-bibliothèque de mutants à insertion de transposons (mutants tn) pour identifier des régulateurs transcriptionnels (RT) impliqués dans la résistance aux antibiotiques des biofilms. Treize de ces RT ont été identifiés comme étant potentiellement importants pour la résistance intrinsèque aux antibiotiques. Parmi ces RT, le mutant tn PA1759 s'est distingué par son phénotype de biofilm susceptibilité aux antibiotiques le plus fort. PA1759 se trouve dans un opéron avec PA1760, donc un mutant à double délétion Δ*PA1759-60* a été construit et analysé. Comparé au biofilm du type sauvage (WT), le mutant Δ*PA1759-60* est quatre fois plus sensible à la Tobramycine (Tb) lorsque son biofilm est exposé aux antibiotiques. Cela suggère que PA1759-60 est un régulateur important de la résistance aux antibiotiques, ce qui nécessite des recherches supplémentaires sur ses mécanismes et son potentiel en tant que cible thérapeutique.

Cette recherche visait à analyser le mutant Δ*PA1759-60* afin de déterminer ses capacités de croissance et de formation de biofilms dans des conditions aérobies ainsi qu’anaérobies, en comparaison avec le WT. Étant donné que PA réside souvent dans des environnements

anaérobies, comme dans les poumons des patients atteints de FK, la caractérisation sous ces deux conditions est importante pour évaluer les résultats cliniques potentiels. Le mutant Δ*PA1759-60* a montré une croissance et une formation de biofilm considérablement réduites par rapport au type sauvage dans des conditions anaérobies, ce qui est cohérent avec les observations antérieures dans des conditions aérobies. Ces résultats soulignent la diminution de la formation de biofilms par Δ*PA1759-60*, fournissant des informations utiles pour le développement futur de thérapies ciblées contre les infections à PA dans des conditions anaérobies.

Acknowledgements

I am immensely thankful to my supervisor, Dr. Thien-Fah Mah, for her invaluable guidance, unwavering support, and continuous encouragement throughout my journey in completing this master's thesis. Her expertise, patience, and constructive feedback, along with the collaborative efforts of my dedicated lab mates, have been instrumental in shaping this work. I would also like to extend a special thanks to my co-supervisor, Dr. Francois- Xavier Campbell-Valois, whose expertise and guidance have enriched this journey significantly.

To my dear mother, Fabiola Batistin, your love, boundless encouragement, and endless sacrifices have been the cornerstone of my journey. Your belief in me, even when I doubted myself, has been a guiding light. Your strength and resilience inspire me every day. I am forever grateful for your nurturing presence and support.

To my beloved father, Reinaldo Burian, your wisdom, guidance, and love have shaped me into the person I am today. Your belief in my abilities and your constant encouragement have been a source of strength throughout this academic pursuit. Your sacrifices and dedication to my success have not gone unnoticed, and I am deeply grateful for everything you have done for me. have shaped me into the person I am today.

To my brother, Eduardo Burian, may you find inspiration in my journey. Your presence and support have meant the world to me. I hope that my accomplishments serve as a beacon of inspiration for you to pursue your dreams fearlessly.

To my in-laws, Shawn and Theresa Simpson, Patricia and Bruce Harrington, your understanding, support, and encouragement have meant the world to me. Your belief in me has

been a source of motivation and strength. I would also like to extend my gratitude to my friends for their support and encouragement throughout this academic endeavor.

Last but certainly not least, I extend my heartfelt thanks to my beloved Michael Simpson. Your unwavering love, endless patience, and support have been my rock during the highs and lows of this thesis journey. Your belief in me never faltered, and for that, I am eternally grateful. And to our beloved cats, who provided comfort, companionship, and endless joy throughout this journey, thank you for your unconditional love and support.

With love and gratitude,

Heloisa Burian

Table of Contents

List of abbreviations

PA = *Pseudomonas aeruginosa*

PA14 = strain UCBPP-PA14, the wildtype strain used in this work

WT = Wild Type

CF= Cystic Fibrosis

TRs = Transcriptional Regulators

Tn-mutant = Transposon-insertion mutant

Tb = Tobramycin

OD600 = Optical Density at 600 nm

OD595= Optical Density at 595 nm

LB = Luria-Bertani broth

LBN= Luria-Bertani broth supplemented with potassium nitrate

M63 = Minimal medium

M63N= Minimal medium supplemented with potassium nitrate

CV = 0.1% Crystal Violet

1.0 Introduction

In 2019, the Centers for Disease Control and Prevention (CDC) estimated that more than 2.8 million antibiotic resistance infections lead to over 35,000 deaths in the United States (Centers for Disease Control and Prevention, 2019).

Antibiotic resistance is a bacteria's ability to resist the effects of antibiotics and is classified by how microorganisms are capable of adapting and proliferating in the presence of antibiotics that used to negatively affect them (Dadgostar, 2019). If antibiotics can no longer be used as a therapy against bacterial infections, these infections can result in severe diseases, extended hospital stays, rises in healthcare expenses, and result in death (Dadgostar, 2019). As a result, antibiotic resistance has become a major problem in the 21st century (Prestinaci et al., 2015).

In Canada, the Canadian Antimicrobial Resistance Surveillance System (CARSS) is a national program managed by the Public Health Agency of Canada (PHAC) that monitors trends of antimicrobial resistance and antimicrobial usage across the country. CARSS gathers and analyzes data from various sources, and it annually provides reports that highlight antimicrobial resistance trends and emerging areas of concern (Public Health Agency of Canada 2024, Rudnick et al., 2022). In their 2024 report, CARSS highlighted the alarming trajectory of antimicrobial resistance, as it is projected to increase drastically by 2050, with an estimated number of potential deaths reaching 14,000 annually. The PHAC continues to emphasize the importance of improving antibiotic surveillance, strengthening antimicrobial stewardship programs and raise public awareness on the matter (Public Health Agency of Canada, 2024).

Pseudomonas aeruginosa (PA) is a gram-negative bacterium that is known to cause serious bacterial infections that are linked to high mortality rates (Murray et al., 2022). The World Health Organization (WHO), in their 2024 report on the Bacterial Priority Pathogens List (BPPL), highlighted PA as part of the critical category of multidrug resistant bacteria, which is particularly hazardous in hospitals due to being highly unaffected by antibiotic treatments (Reig et al., 2022, World Health Organization, 2024). PA is especially recognized for causing chronic infections due to its ability to form biofilms, clusters of bacteria surrounded by a self-produced extracellular matrix. It is important to note that cells in a biofilm are very resistant to the effects of antimicrobial agents, due to the bacteria within the biofilm being protected by a matrix that limits antibiotic penetration (Mah et al., 2003). This, combined with the bacteria having multiple mechanisms of defense, makes antibiotic treatment extremely difficult or impossible (Mah et al., 2003).

As the most common pathogen in the CF microbiome, PA can promote chronic lung infections in individuals with CF (Acosta et al., 2020). The environment within the CF lung is complex and poses significant challenges to the diversity of bacteria and microorganisms that inhabit it (Bhagirath et al., 2016). Within this environment, and due to the thick mucus typical of CF, there exists anaerobic spaces that can contribute to disease progression and the persistence of biofilms. These low-oxygen areas then provide conditions for PA to settle, eventually forming and growing biofilms. (Thornton and Surette, 2021).

Historically, the most commonly prescribed antibiotics to treat PA infections in cystic fibrosis (CF) were aminoglycosides, such as Tobramycin (Tb) (Kaushik et al., 2016). However, treatment strategies have evolved, and a broader variety of antibiotic is now utilized. Currently, options include antibiotic agents such as beta-lactams, cephalosporins, fluoroquinolones,

carbapenems, and aminoglycosides which still remains an important therapeutic option for treating PA infections (Tamma et al., 2024).

1.1 *Pseudomonas aeruginosa* (PA)

PA is a rod-shaped, gram-negative bacteria that is widely distributed in the environment. Due to its exceptional metabolic adaptability, PA has the ability to thrive in aerobic, hypoxic, and anaerobic conditions. PA is an opportunistic pathogen that can affect humans and other organisms, often causing disease when the host's immune system is weakened (Chandler et al., 2019).

PA being resistant to many antibiotics, and is also amongst one of the most frequent causes of hospital-acquired infections that can result in acute and chronic illness. Patients undergoing organ transplants, or suffering from cystic fibrosis, acute leukemia, and burn injuries are more likely to get infected with this pathogen (Bodey et al., 1983).

In many cases, PA infections do not improve with prolonged antibiotic treatment. This phenomenon is partially explained by the fact that in chronic infections in the CF lung, PA exists in a polysaccharide-based, antibiotic-resistant biofilm consisting of bacterial clusters, making treatment nearly impossible (Stover et al., 2000).

While numerous PAs isolates have been identified and published on, two of the strains that are most commonly used to evaluate innovative treatments and comprehend the genetic makeup of the bacteria are *Pseudomonas aeruginosa* PAO1 and PA14. The PAO1 strain is a

variation of "*Pseudomonas aeruginosa strain 1*," which was first discovered in a patient's wound isolate in 1954 in Australia (Chandler et al., 2019).

PA14 (also called UCBPP-PA14) is used as the primary pathogen in the Mah lab because it is significantly more virulent in both plants and animals, compared to PAO1 (Rahme et al., 1995). PA14 was first isolated from burn wound patients at a Pennsylvania hospital in the 1970's (Schroth et al., 1977, Mathee, 2018). This originated a study on the relationship between plant pathogens and human infections, in which PA14 was used as the preferred model for researching the pathogenicity and virulence of PA. PA14 has since evolved into a highly favored model for pathogenicity and severe PA infections (Grace et al., 2022). The increased virulence of PA14 is attributed to the presence of two pathogenicity islands, PAPI-1 and PAPI-2. These DNA segments contain genes that enhance the bacterium's virulence, thus causing more severe infection in its hosts. It is important to note that these pathogenicity islands are unique to PA14, and that they are absent from the PAO1 genome. This highlights the main genetic differences that contribute to the virulence disparity between these two PA strains (Grace et al., 2022, Harrison et al., 2010).

1.2 Antibiotic Resistance

Antibiotic resistance is a major worldwide health issue; it can happen in a variety of ways, including the horizontal gene transfer of resistance genes, as well as the generation of a resistance gene through mutation (Martinez and Baquero, 2000). Indeed, bacteria are more likely to survive and proliferate if these mutations can offer a competitive edge over antibiotics (Bengtsson-Palme et al., 2018).

In order to withstand the effects of several antibiotics, PA strains use both acquired and intrinsic resistance mechanisms. The most prevalent causes of acquired resistance are from mutations or the exchange of antibiotic resistance genes. For example, some PA isolates may have mutations in the *amp*C gene that can lead to the overproduction of beta-lactamases, resulting in an increase resistance towards beta-lactam antibiotics (Pang et al.,2019). Acquired resistance further contributes to the establishment of multidrug-resistant strains, making it more difficult to eliminate pathogens and resulting in more persistent diseases (Pang et al., 2019). Intrinsic resistance relies on wild-type genes and the bacterial cell's innate features (Fajardo et al., 2008). Examples of PA's intrinsic resistance mechanisms include limited outer membrane permeability, and the expression of efflux pumps, such as *mexAB-oprM*, that remove antibiotics from the cell. Gene encoding antibiotic-inactivating enzyme, provided they are not associated with horizontal transfer elements is also an intrinsic mechanism (Pang et al., 2019).

Antibiotic resistance in PA biofilms can occur when certain genes, such as *ndvB*, tss*C1*, *PA1874-77*, *PA2070*, *PA5033*, *tctED*, are expressed in the PA genome. These genes are all known to contribute to intrinsic mechanisms of resistance. (Beaudoin et al., 2012; Hall and Mah, 2017; Mah et al., 2003; Taylor et al., 2019; Zhang et al., 2011; Zhang et al., 2013; Zhang and Mah, 2008). These genes have also been linked to biofilm-mediated antibiotic resistance, and the function of some have been well-characterized. Amongst the genes with known functions are the *ndvB* gene, that encodes a protein involved in the production of cyclic glucans, which plays a role in antibiotic sequestration (Mah et al., 2003), *PA1874-77* genes that encode biofilm specific multidrug efflux pumps (Zhang and Mah, 2008), and *tctED* genes that encodes a two-component system TctD-TctE, which regulates the uptake of citric acid and regulates biofilm formation in response to it (Taylor et al., 2019).

The mechanisms of resistance of the other genes remain unknown, despite there being some predictions about their gene products. For instance, *tssC1* encodes a component of a Type VI secretion system but its exact role in resistance has not been uncovered (Zhang et al., 2011). The *PA2070* gene product is predicted to be part of a TonB-dependent receptor and PA5033 is classified as a hypothetical protein (Zhang et al., 2013; Hall and Mah, 2017) and their contributions to biofilm resistance are not clear.

1.3 Cystic Fibrosis (CF)

Cystic fibrosis (CF) arises from genetic changes that impact both copies of the cystic fibrosis transmembrane conductance regulator (CFTR) gene (Davies, 2002). The abnormal buildup of thick, sticky mucus in CF airways is caused by either dysfunctional or absent CFTR. This mucus impedes the clearance by mucociliary cells, lessens the absorption of bacteria by lung epithelial cells, blocks antimicrobial peptides, and makes it easier for microbial pathogens to colonize the respiratory tract (Davies, 2002; Bhagirath et al., 2016). As a result, infections can become quite common in CF patients' lungs due to the ability of microorganisms to proliferate and form colonies there. Within the thick mucus secretions characteristic of CF lungs, hypoxic and anaerobic spaces exist that support the growth of anaerobic bacteria. PA further influences this environment by forming biofilms and utilizing nitrate to support anaerobic growth. The growth of bacteria within these anaerobic spaces may be indicative of disease progression and may contribute to disease within the airways (Thornton and Surette, 2021).

The CF microbiome refers to the complex community of various microorganisms residing in the lungs of individuals with CF. The thick mucus present in the CF lung

consequently supplies bacteria with an environment containing nutrients that it needs to grow and proliferate (Palmer et al., 2007).

Reports on the predominant pathogen in the CF microbiome indicates it to be PA, an organism that can thrive in the anaerobic conditions. In the CF microbiome, the PA biofilm strains that are resistant to antibiotics may evolve because of the difficulty in eliminating the biofilm. The CF airway is now recognized to be the habitat for many different types of bacteria, such as *Staphylococcus aureus*, *Haemophilus influenzae* and *Stenotrophomonas maltophilia*, and obligate anaerobes like *Prevotella* and *Veillonella* (Thornton and Surette, 2021). These bacterial species are known to interact with PA in ways that can enhance the expression of virulence and resistance genes (Thornton and Surette, 2021).

For instance, *S.aureus* is an early colonizer in CF patients, typically found in younger individuals, whereas PA predominates in adult patients (Fischer et al., 2021). These two bacterial species can either compete with each other through the production of antimicrobials, coexist within the same biofilms, or PA can outcompete *S.aureus* and other bacteria in biofilms through quorum sensing regulations (Hotterbeekx et al., 2017). While these organisms are not exclusive to CF, the unique microbiome of the CF lung creates an environment where the interactions between these species influences disease progression and development of PA's virulence and resistance (Reece et al., 2021).

Infections by PA are particularly common in CF patients. It has been reported that 60–80% of CF patients have suffered from PA infections (Acosta et al., 2020). Antibiotic therapy alone cannot cure a chronic PA infection, which causes lung function to deteriorate and can ultimately result in death of CF patients (Pang et al., 2019).

1.4 Biofilms

Similar to other bacteria, PA is known for being able to grow in two different forms: as unicellular or planktonic cells, in which the cells are free to circulate in the environment, and in multicellular (sessile) communities, called biofilms (Berlanga and Guerrero, 2016). The cells that are inside a biofilm are encased in a self-produced matrix, that typically consist of lipids, proteins, extracellular DNA and exopolysaccharides, making biofilms a microbial colony that clings to biotic and abiotic surfaces (Hobley et al., 2015). Due to their role in the pathogenesis of various bacterial infections that are challenging to treat with antibiotics, biofilms are significant from a medical standpoint (Berlanga and Guerrero, 2016).

The highly controlled biofilm formation developmental process is influenced by a variety of environmental and genetic variables (Alotaibi, 2021). According to the traditional developmental theory of biofilm formation, several environmental stimuli cause motile planktonic cells to adhere to a surface and begin forming biofilms (Donlan, 2002).

Biofilm formation in PA begins with free-swimming planktonic cells. The process starts when these cells undergo initial attachment by adhering to a surface. At this stage, cells that are motile then begin to aggregate and accumulate, leading to the formation of a microcolony. Following the development of microcolonies, the biofilm enters a maturation phase in which macrocolonies develop, this step requires both growth and biofilm formation genes. This is where the most significant growth phase happens and is facilitated by the production of a matrix, which not only helps the cell adhere more securely to the surface but also provides nutrients and protection. Lastly the biofilm undergoes detachment and cell dispersion, during this phase cells may exit the biofilm reverting to their planktonic state. These dispersed cells can then remain

free-moving planktonic cells or start a new biofilm continuing the cycle (Alotaibi, 2021) (Figure 1). In laboratory conditions, PA primarily forms biofilms at the air-liquid interface when growing aerobically, while in anaerobic conditions, PA forms biofilms at the bottom of wells (O'May et al., 2006). Interestingly, although PA can form biofilms in both aerobic and anaerobic environments, a report indicates that biofilms may be more robust and denser under anaerobic conditions (Yoon et al., 2011; Furiga et al., 2015).

It is important to note that an essential step in the initial attachment of cells during biofilm formation involves the roles of the flagellum and type IV pili in planktonic cells. The flagellum is essential for cell motility, allowing cells to swim to the air-liquid interface and attach to surfaces. Once the cell is attached, type IV pili enables twitching motility, which is necessary for movement along the surface and formation of microcolonies. Both structures are important for biofilm formation (Conrad et al., 2011).

When studying biofilms in a 96-microtiter plate, the mutant Δ*flgK* is often used as the negative control for biofilm formation. This mutant is well-known for its inability to form biofilms under aerobic conditions due to its flagellar mutation. Without a functional flagellum, the strain exhibits significantly reduced motility making it difficult to reach the air-liquid interface where aerobic biofilms typically form, preventing cell attachment to the well surfaces (O'Toole and Kolter, 1998). To our knowledge, this is the first study to demonstrate that under anaerobic conditions, the Δ*flgK* mutant can form biofilms at the bottom of the wells.

The shift from planktonic to biofilm growth is significant because biofilm cells form a high-density community in which they are exposed to diverse environmental conditions. As a result, different conditions exist within various parts of the biofilm, such as gradients of nutrient availability, oxygen levels and pH levels (Jefferson, 2004). These gradients exist inside the

biofilm are due to the diminishing supply of nutrients that are located towards the center of the biofilm. The cells that are at the edge of the biofilm are able to take advantage of available nutrients, while cells that reside in the center of the biofilm have to reduce their metabolic processes to compete for the limited supply of nutrients (Stevanovic et al., 2022). This often results in a slower doubling rate (Shree et al., 2023). This diversity allows bacteria in different areas of the same biofilm to exhibit distinct metabolic processes and express diverse gene products (Jefferson, 2004).

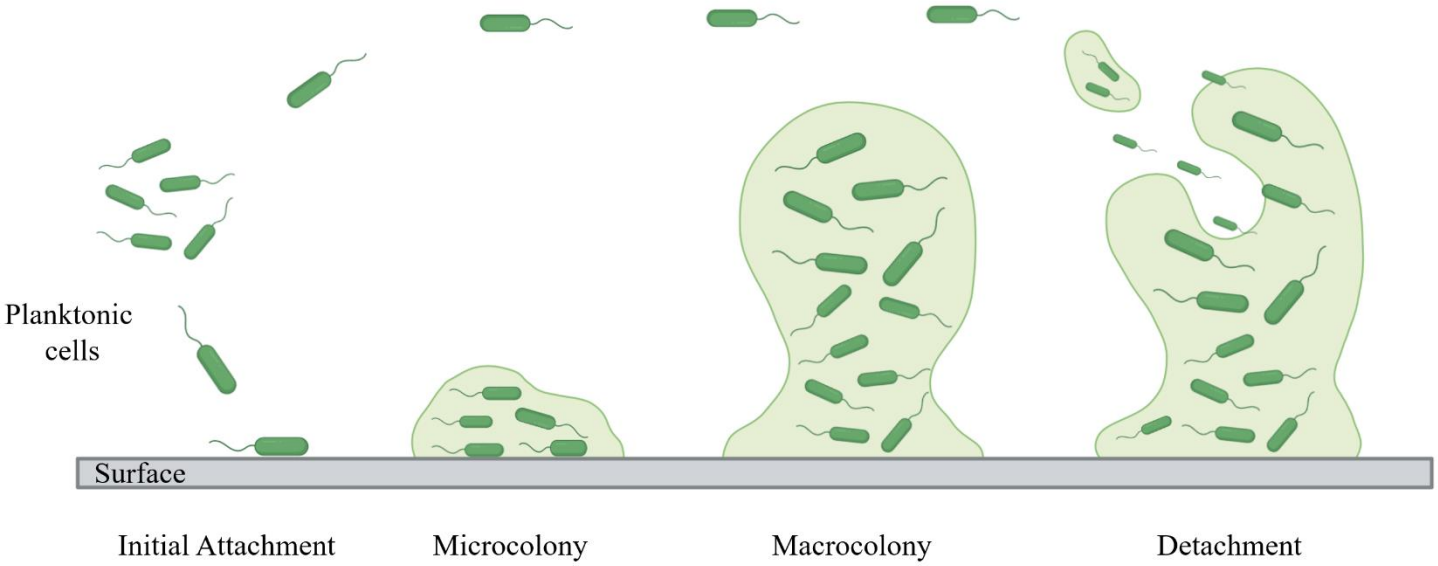

Figure 1: Simplified schematic of the main stages involved in the development of biofilms (Maunders and Welch, 2017). Initial attachment to a surface requires cells to be present and able to attach. Surface motility is required for the formation of microcolonies. Both growth and biofilm formation genes are required for the development of microcolonies. Detachment of cells from biofilm and dispersion of planktonic cells can re-start the cycle and proceed to form a new biofilm. Figure created using Biorender.

1.5 Antibiotic resistance in Biofilms

Biofilms have the ability to create a protective matrix that makes them more resistant to antibiotics. Furthermore, the expression of genes that are unique to biofilms, can then increase the ability of the cells within the biofilm to protect themselves from antimicrobial agents like antibiotics.

When applied, antibiotics can be less effective due to a variety of factors, including slower growth rate and interactions with the matrix that can diminish the antibiotic diffusion into the biofilm, and the activity of efflux pumps, which can more easily reduce the cytoplasmic antibiotic concentration below the toxicity threshold (Ferrer-Espada et al., 2019). Additionally, the Mah lab has studied several genes that encode different mechanisms of resistance, all in which are more highly expressed in biofilms. These genes are *ndvB,* tss*C1, PA1874-77, PA2070, PA5033* and *tctED* and, as described in Section 1.2, they contribute to different mechanisms of resistance. (Beaudoin et al., 2012; Hall and Mah, 2017; Mah et al., 2003; Taylor et al., 2019; Zhang et al., 2011; Zhang and Mah, 2008).

The importance of these genes for biofilm antibiotic resistance, coupled with the fact that these genes are more highly expressed in biofilms, has led to the hypothesis that specific transcriptional regulators (TRs) may be involved in controlling the expression of these genes. Thus, these TRs would be of great interest because of their ability to influence antibiotic resistance.

1.6 Transcriptional regulators (TRs)

Transcriptional regulators (TRs) are proteins that can control the expression of specific genes by turning on or off their transcription (Sánchez-Jiménez et al., 2023). The most abundant family type of bacterial TRs, found in both gram-negative and gram-positive bacteria, are the LysR-type. These TRs are known to activate or repress the transcription of important gene involved in regulating essential cellular functions and certain genes responsible for motility, virulence, quorum sensing, and antibiotic resistance (Reen et al., 2013).

In the context of antibiotic resistance, TRs can activate genes that help bacteria survive in the presence of antibiotics. However, for biofilm-specific antibiotic resistance, the roles of TRs remain unclear as there is limited understanding of how these regulators contribute to mechanisms that make biofilms more resistant to antibiotics (Grooters et al., 2024). In PA one particular TR, BrlR (PA4878), has been identified to be involved in biofilm antibiotic resistance (Liao and Sauer, 2012).

BrlR is a TR specific to PA biofilms, as its protein is present in cells within biofilms but not when in a planktonic state. It belongs to the MerR-like family, binding to DNA and activating the expression of multidrug efflux pump genes, including *mexAB-oprM* and *mexEF-oprN*, making it difficult for antibiotics to penetrate and destroys the bacteria (Liao and Sauer, 2012).

1.7 Previous work in the Mah Lab

The Mah lab has focused on studying individual genes crucial for antibiotic resistance (Beaudoin et al., 2012; Hall and Mah, 2017; Mah et al., 2003; Taylor et al., 2019; Zhang et al., 2011; Zhang and Mah, 2008). In recent years, there has been a shift towards understanding how the expression of genes crucial for antibiotic resistance is regulated. This focus is driven by the global antibiotic resistance crisis, where resistance has been seen in all clinically used antibiotics, while the development of new antibiotics has drastically slowed. By better understanding the mechanisms of intrinsic resistance, we can create novel approaches to eliminate antibiotic-resistant infections.

Previous research in the Mah Lab, conducted by Clayton Hall, involved compiling a sub-library of transposon-insertion mutants (tn-mutants) representing the predicted TRs in the PA genome. This sub-library was created based on the broader library described by Liberati et al., 2006, and it was comprised of tn-mutants representing most of the proposed TRs in PA that were deemed important for biofilm-based antibiotic resistance. During the screening process, biofilms formed by these mutants were exposed to sub-lethal concentrations of Tb, and after 24 hours the bacteria was assessed for survival. Thirteen such TRs were identified. The thirteen tn-mutants were shown to not have a growth deficiency, nor a biofilm formation deficiency as compared to the WT counterpart. Hall also conducted one round of biofilm antibiotic susceptibility assays and observed that they were more susceptible to Tb than the WT. Hall continued to focus mainly on the tn-mutant of PA1759 since it had the strongest biofilm-specific antibiotic susceptibility phenotype.

Antibiotic resistance assays were done using Tb, historically a commonly prescribed aminoglycoside antibiotic to treat infections caused by PA (Kaushik et al., 2016). The

mechanism of action of this antibiotic involves binding to lipopolysaccharides present on the outer membrane of gram-negative bacterium to enable an entryway into their cytoplasm (Bulitta et al., 2015; Krause et al., 2016). Once inside the cytoplasm, it disrupts the bacterial protein synthesis by interfering with the 30S ribosomal subunit, causing errors in mRNA translation. This ultimately inhibits the production of essential proteins required for bacterial growth. (Mangiaterra et al., 2023).

1.8 PA14 Δ*1759-60*

In order to further analyze these TRs, it was important to determine the percentage identity at the protein level between PA1759 and PA1760. Using the protein BLAST (Basic Local Alignment Search Tool) (Altschul et al., 1990) a pairwise sequence comparison of PA1759 and PA1760 was performed. This analysis showed that the two proteins share 29.41% identity and 48% similarity in their amino acid sequences. While PA1759 and PA1760 have some similarities at the protein level, their sequence composition is significantly different. This suggests that, while they might share some functional or structural elements, they are not identical proteins.

The genes encoding PA1759 and PA1760 were predicted to form an operon using the Pseudomonas Genome Database (Lee et al., 2006), which uses the Database of Prokaryotic Operons (DOOR) (Winsor et al., 2011). I have independently verified this prediction by using the Operon Mapper tool (Taboada et al., 2018) and the Bacterial Promoter Prediction Program (BPROM) (Solovyev and Salamov, 2011), confirming the operon structure of these genes. These genes are likely to encode TRs, as their proteins are predicted to be part of the MalT domain

family type of TRs, with an ATP binding domain in the N-terminus and a LuxR DNA-binding domain in the C-terminus. The ATP binding domain suggests that it uses ATP as an energy source or to signal activation in the protein (Danot, 2001). However, while these proteins are part of the MalT domain family, a BLAST search comparing the PA1759-60 protein sequences with MalT from *Escherichia coli* revealed a low sequence identity, indicating that they are not likely orthologs of MalT. Specifically, PA1759-60 lacked homology with central ligand binding domain of MalT suggesting that it is unlikely that PA1759 and PA1760 bind to maltotriose, thus distinguishing them functionally from MalT. Their presence in the same operon suggests that their expression is co-regulated and potentially have related functions (Figure 2).

Li Zhang (former technician in the Mah Lab) constructed both single deletion mutants of PA1759 and PA1760, as well the double deletion mutant of PA1759-60 (Figure 2). This process involved designing PCR primers to amplify and generate fragments that were homologous to the regions flanking the target genes. These fragments were then purified and digested with the appropriate restriction enzymes nucleases and ligated into a plasmid with a selectable marker. The deletion constructs were then introduced to PA through transformation followed by homologous recombination to replace the target sequences (Figure 3). PCR was used to confirm if the deletion protocol was successful. Li Zhang completed an initial analysis of these deletion mutants, performing growth assays, biofilm formation assays and antibiotic resistance assays.

The single deletion of either gene does not have a noticeable antibiotic-susceptibility phenotype, however, deleting both genes together makes the biofilm more susceptible to Tb. While the Δ*PA1759-60* mutant displayed decrease in growth and biofilm formation under aerobic conditions, it was determined that the Δ*PA1759-60* mutant was four times more susceptible to Tb when its biofilm is exposed to antibiotics than the WT. Given that the single

deletions of either PA1759 or PA1760 do not result in a noticeable antibiotic susceptibility phenotype, but the double deletion increases biofilm susceptibility to Tb, this suggests that PA1759 and PA1760 might be functionally redundant**.**

These data suggested that these TRs warrant further investigation. Since this mutant's growth abilities, biofilm formation, and antibiotic susceptibility have all been examined in aerobic conditions in the Mah Lab, it was of interest to determine its phenotype under anaerobic conditions, a condition where PA finds itself in CF patients.

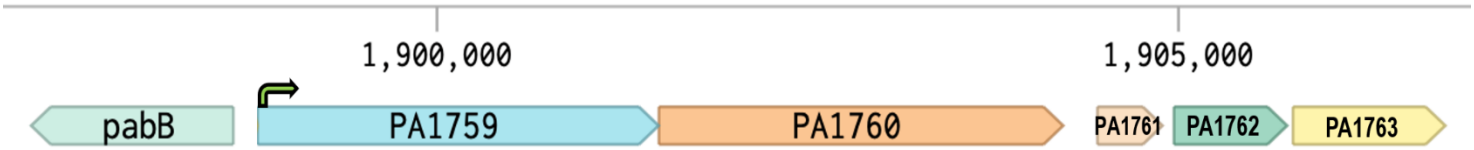

Figure 2: Schematic representation of the *PA1759-60* operon in *Pseudomonas aeruginosa.* The diagram shows the operon structure containing the genes PA1759 and PA1760. The arrow corresponds to the predicted promoter for these genes. The upstream gene is *pabB* and downstream genes are uncharacterized. For simplicity, the PAO1 gene nomenclature is used in this schematic, but the corresponding PA14 genes are PA14_41800 and PA14_41810. Source: *Pseudomonas* Genome Database (Lee et al., 2006; Winsor et al., 2016). Figure created using Benchling.

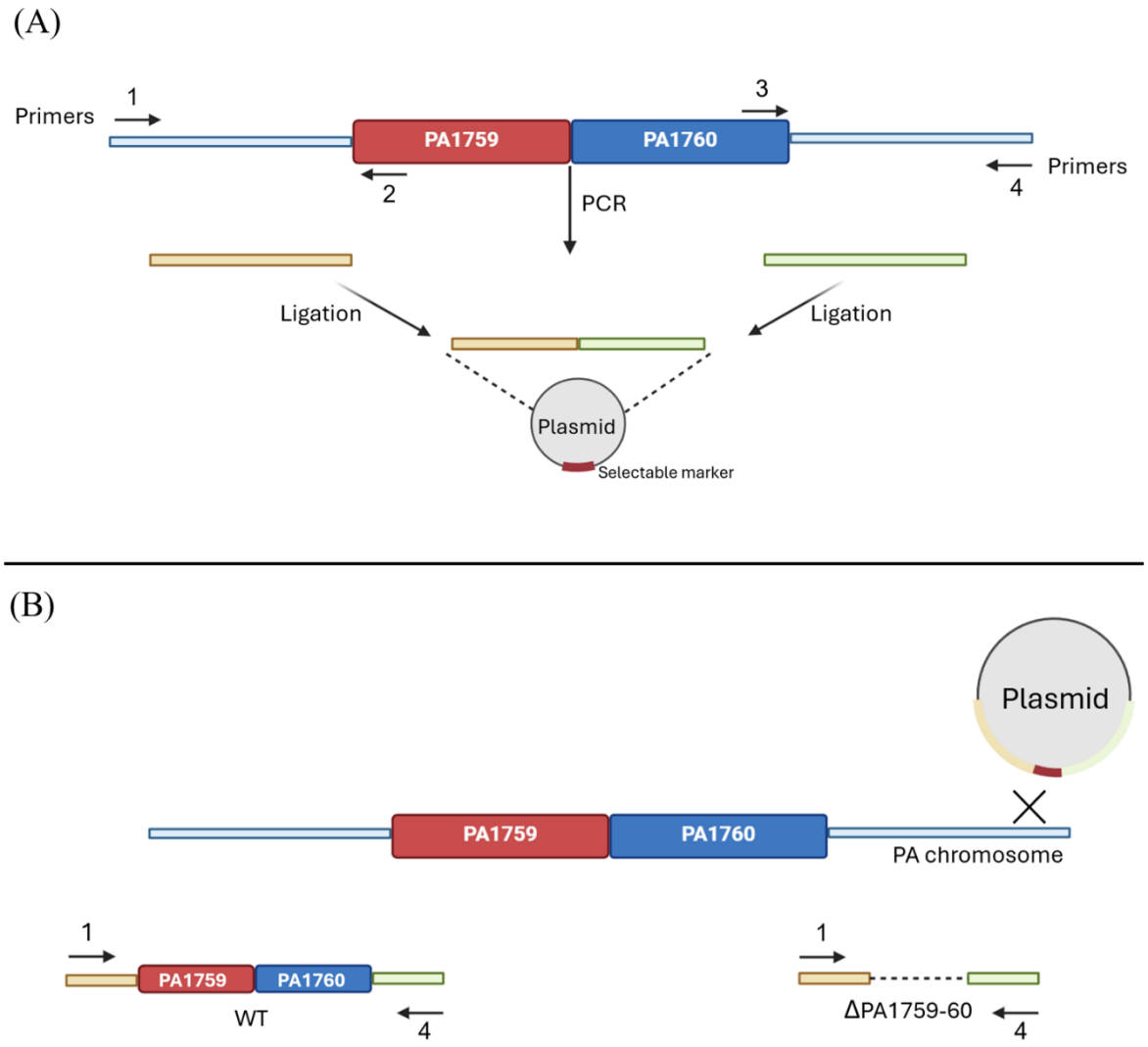

Figure 3: Schematic representation of the protocol used to create the deletion construct of PA1759 and PA1760 constructed by Li Zhang. (A) Primers were used to PCR amplify the upstream region of PA1759 and downstream region of PA1760, these fragments were purified, digested by the appropriate restriction enzymes nucleases and ligated into the appropriate plasmid. (B) The deletion construct, as part of a stable plasmid, was introduced into PA. Homologous recombination into the chromosome and subsequent resolution of the merodiploid yielded the desired mutant. Figure created using Biorender.

1.9 Objectives and Hypothesis

The objectives of this research are to compare the growth of Δ*PA1759-60* to the Wild-type (WT) strain under anaerobic conditions, assess the ability of the mutant strain to form biofilms compared to the WT under anaerobic conditions, and compare any growth or biofilm formation defects in the presence and absence of oxygen.

With this focus, I have developed a hypothesis that:

P.aeruginosa Δ*PA1759-60* displays decreased growth and ability to form biofilms compared to the Wild-type strain when grown under anaerobic conditions

The rationale for assessing the phenotype of Δ*PA1759-60* under anaerobic conditions is based on the recognition that PA often exists in anaerobic environments, most notably within the CF lung, despite this there is still very limited research on biofilms in anaerobic conditions.

Preliminary data shows that under aerobic conditions, Δ*PA1759-60* does not grow or form biofilm as well as the WT. Given that anaerobic conditions are generally more stressful for bacterial cells, the effects observed in aerobic conditions for Δ*PA1759-60* might be further intensified under the anaerobic conditions. By examining Δ*PA1759-60* under anaerobic conditions, I aim to gain insights into its growth abilities and biofilm formation.

2.0 Materials and Methods

2.1 Bacterial Strains

The laboratory strains used in this research were PA14 (UCBPP-PA14) (Lee et al., 2006) (Schroth et al.,1977), Δ*PA1759-60* (constructed by Li Zhang), and Δ*flgK* (O'Toole and Kolter, 1998). These mutant strains used are isogenic to PA14, with the only genetic differences being the deletions of the *PA1759-60* and *flgK* genes, respectively.

The mutant Δ*flgK* is commonly used as a negative control in aerobic biofilm formation assays. Its lack in a functional flagellum results in reduced motility, preventing it from swimming to the air-liquid interact where aerobic biofilm typically forms (O'Toole and Kolter, 1998).

Spectrophotometry measurements

The optical density (OD) of bacterial cultures was measured at 600 nm (OD600) using a (Bio-Rad Smartspec 3000 UV/VIS) spectrophotometer. Prior to each measurement, the spectrophotometer was calibrated by using a blank cuvette containing the corresponding growth medium to zero the instrument, ensuring that the recorded OD values reflected only bacterial turbidity.

2.2 Aerobic Growth Assay

Growth curves were carried out to compare the growth kinetics of the Δ*PA1759-60* mutant to the WT strain, which served as the positive control. The mutant and WT strains were first inoculated in Luria-Bertani (LB) broth and then incubated overnight for 16 hours. The next day the optical density (OD) of the overnight bacterial culture was measured at 600 nm (OD600), and found to be approximately 1.5, the strains were then subcultured, transferring 50 µl of the overnight culture to new test tubes containing 5 mL of LB and incubated for an additional 5 hours. LB was chosen for this assay as it is a nutrient-rich medium as it promotes rapid planktonic growth, making it excellent for assessing overall bacterial growth rates. At the end of the subculture incubation period, the OD was measured at OD600 and found to be approximately 0.5. The cultures were then diluted to match the OD of the WT strain to ensure uniformity across all samples.

Using a 96-well microtiter plate, 90 µl of LB was added to each well for the technical replicates of the WT, Δ*PA1759-60,* and a blank control. Then 10 µl of the subculture for each strain was added to these wells, making the total volume in each well 100 µl.

Following that, the 96-well microtiter plate was put in a plate reader (BioTek Synergy H1 Multi-Mode Plate Reader) and shaken while it was incubated at 37°C. Throughout the course of the 18 hour experiment, absorbance at OD600 nm was measured every 30 minutes using the Gen5 program. Upon completion of the experiment, the growth of the mutant was compared to the WT. As part of the protocol, no negative control was included in this experimental design, however, ideally a negative control would involve using fresh LB culture without any bacteria to

account for potential contamination. For this experiment, three independent biological replicate experiments were performed, and each biological replicate included four technical replicates per strain.

2.3 Aerobic Biofilm Formation Assay

A biofilm test was performed using the Δ*PA1759-60* mutant, WT as the positive control, Δ*flgK* as the negative control (O'Toole and Kolter, 1998), and a blank which consisted of wells containing only M63 medium without bacteria that underwent the same experimental steps as the other strains. The strains were initially inoculated in 5 mL of LB medium and incubated for 16 hours at 37°C. The next day the OD600 of each strain was measured and the cultures were diluted into M63 medium to match the OD 0.1 of the WT strain to ensure uniformity across all samples. The use of M63 as a minimum medium was chosen for this assay as it simulates nutritional stress and encourages the sessile behavior required for biofilm development (O'Toole, 2011). Following this, 10 µl of each culture was mixed with 490 µl of 1X M63 medium in Eppendorf tubes, resulting in a 1:50 dilution. 100 µl of these mixtures were then inoculated into a 96-well microtiter plate, with each strain having four replicate wells, including controls. Three independent biological replicate experiments were performed, and each biological replicate included four technical replicates per strain.

The plate was incubated for 24 hours at 37°C. After incubation, the plate was taken from the incubator, and the supernatant unattached cells were discarded by flipping the plate and shaking the liquid into a waste container. The plate was then submerged in clean water to remove

any cells that did not attach to the walls of the wells. After shaking out the excess water, the plate was blotted on a paper towel to absorb any remaining water in the wells.

Each well containing the strains received a 15-minute incubation with 125 µl of 0.1% Crystal Violet (CV) solution at room temperature. To eliminate CV from the wells, the plate was shaken over the waste container before being rinsed in water. Blotting the plate on paper helped remove extra water, cells, and colour. Finally, the plate was allowed to dry overnight.

Quantification of the biofilm was done by resolubilizing the CV in 125 µl of 30% acetic acid for 15 minutes, then absorbance reading at 595 nm was done using a BioTek Synergy H1 Multi-Mode plate reader.

2.4 Anaerobic Growth Assay

A growth curve assay was carried out under anaerobic conditions to compare the growth kinetics of the Δ*PA1759-60* mutant and the WT strain, which served as the positive control. The strains were first inoculated in aerobic conditions in LB medium and incubated for 16 hours at 37°C. The next day the OD of the overnight bacterial culture was measured at 600 nm (OD600) and found to be approximately 1.5. The strains were then subcultured, transferring 50 µl of the overnight culture to new test tubes containing 5 mL of LB medium enriched with potassium nitrate (KNO3), or LBN, which is served as a replacement electron acceptor to compensate for the lack of oxygen, and is a nutrient-rich medium. It promotes rapid planktonic growth, making it excellent for assessing overall bacterial growth rates. The strains were then anaerobically incubated for an additional 5 hours. At the end of the subculture incubation period, the OD was measured at OD600

and found to be approximately 0.5. The cultures were then diluted to match the OD of the WT strain to ensure uniformity across all samples.

Following that, 10 µl of culture for each strain was placed in individual Eppendorf tubes containing 90 µl of LBN, making a total volume of 100 µl. Then this mixture was dispensed into a 96-well microtiter plate. In addition, roughly three drops of baby oil was added to each well that contained the strains, to function as a physical barrier to minimize oxygen exposure and maintain an anaerobic environment throughout the experiment. Additional measures included applying a laminated film cover (Microseal 'B' PCR Plate Sealing Film) to the wells of the 96-well microtiter plate and tightly covering the prepared plate with tape and parafilm to maintain an anaerobic atmosphere. The microtiter plate was then placed in a (BioTek Synergy H1 Multi-Mode) plate reader. The plate was then repeatedly shaken for 18 hours at 37°C, with OD measurements performed every 30 minutes. For this experiment, three independent biological replicate experiments were performed, and each biological replicate included four technical replicates per strain.

2.5 Anaerobic Biofilm Formation Assay

For the anaerobic biofilm experiment, WT (positive control), Δ*PA1759-60* (mutant), and Δ*flgK*, strains were used for this experiment, and a blank (negative control) which consisted of wells containing only M63N medium without bacteria that underwent the same experimental steps as the other strains. These strains were initially inoculated in 5 mL of LB, and incubated for 16 hours at 37°C. The next day the OD600 of each strain was measured, and the cultures were diluted into 1XM63 supplemented with potassium nitrate (KNO3), or M63N medium, to match

the OD 0.1 of the WT strain to ensure uniformity across all samples. The use of M63N as a minimum medium was chosen for this assay as it simulates nutritional stress and encourages the sessile behavior required for biofilm development. Following this, 10 µl of each culture was mixed with 490 µl of M63N, in Eppendorf tubes, resulting in a 1:50 dilution. Then 100 µl of these mixtures were transferred to a 96-well microtiter plate before being put inside the anaerobic chamber (Bactron300 Anaerobic Chamber) for incubation at 37°C for either 24, 48 or 72 hours. For the 24 hour incubation, the plate was removed from the anaerobic chamber, the supernatant was discarded, and the plate was washed three times in a clean water container, to remove non-adherent cells. For the 48 hour incubation, the supernatant was removed after 24 hours in the anaerobic chamber, fresh M63N was added, and it was incubated for another 24 hours, and for the 72 hours incubation, the experiment followed the same procedure, but the supernatant was discarded, and the cells were refreshed with M63N every 24 hours.

After discarding the supernatant at each timepoint, the plates were then stained with 125 µl of 0.1% CV for each well for 15 minutes at room temperature, rinsed with water, and allowed to dry overnight upside down. The same procedure was repeated for the 48 and 72 hour plates.

Quantification of the biofilm was done by resolubilizing the CV in 125 µl of 30% acetic acid for 15 minutes, then absorbance reading at 595 nm was done using a (BioTek Synergy H1 Multi-Mode) plate reader. Three independent biological replicate experiments were performed, and each biological replicate included four technical replicates per strain.

2.6 Statistical Analyses

Growth Assays

Percentage Difference in Optical Density

To compare the growth differences between WT and the Δ*PA1759-60* mutant, at the 10 hour and 17.5 hour timepoints, the percentage difference in optical density (OD) was calculated using the following formula. This analysis was performed using Microsoft Excel (version 2410).

$$\text{Percentage difference (\% diff.)} = \frac{\text{OD}_{\text{WT}} - \text{OD}_{\Delta\text{PA1759-60}}}{\text{OD}_{\text{WT}}} \text{ x } 100$$

Two tailed t-test

A two tailed t-test was conducted to assess whether there were statistically significant differences in growth between the WT and the Δ*PA1759-60* mutant, at the 10 hour and 17.5 hour timepoints. The test assumes that the data is normally distributed and that the two groups are independent. The significance level of p-value being $p < 0.05$ was used to determine statistical significance (Xu et al., 2017). This analysis was performed using Microsoft Excel (version 2410).

Biofilm Formation – Crystal Violet Assays

One-way ANOVA

A one-way ANOVA was performed to determine if there were significant differences in the mean OD595 quantification values of the crystal violet assay amongst the three groups: WT, Δ*PA1759-60* and the Δ*flgK*. This statistical test assess the variance within and between groups to determine if there is a statistically significant difference in the means of the groups. A significance level of p-value being $p < 0.05$ was used to determine if differences were significant. However, this test does not specify which pair groups are different from each other, only that at least one pair is different (Codjo et al., 2024). This analysis was performed using Microsoft Excel (version 2410).

Post-hoc Tukey's HSD test

Following the one-way ANOVA, a post-hoc Tukey's HSD (honest significant difference) test was performed to identify which specific pairs of groups (WT, Δ*PA1759-60* and Δ*flgK*) were significantly different from each other. This test provides pairwise comparisons and indicates its significant differences (Codjo et al., 2024). This analysis was performed using Microsoft Excel (version 2410) and Statistics Kingdom (Statistics Kingdom, 2017).

3.0 Results

3.1 Aerobic Growth Assay

A growth assay was performed to assess any potential growth-deficiency phenotype of the Δ*PA1759-60* mutant under aerobic conditions before analyzing its phenotype under anaerobic conditions. The results (Figure 4) demonstrate that the WT exhibited a robust growth under aerobic conditions in LB medium. By contrast, the Δ*PA1759-60* mutant showed a significantly impaired growth compared to the WT.

To provide a more quantitative analysis of the growth curves and allow for a better comparison of the differences in growth, the percentage difference in optical density was calculated between WT and the Δ*PA1759-60* mutant strain at the 10 hour point, and at the 17.5 hour point (Figure 4).

At the 10 hour point the percentage difference for the aerobic growth was that the mutant Δ*PA1759-60* showed a 41.3% lower OD compared to WT and at the 17.5 hour point the mutant showed a 35.5% lower OD compared to the WT. Additionally, a statistical analysis using a two-tailed t-test was performed to compare the difference in growth of the WT and the Δ*PA1759-60* mutant at the 10 hour and 17.5 hour points. The test assumed equal variances and independent samples for both strains.

At the 10 hours, the WT strain (M = 1.00, SD = 0.06) has a significantly higher growth compared to the Δ*PA1759-60* mutant (M = 0.59, SD = 0.01), $t(4) = 10.8$, $p < 0.001$. Similarly at 17.5 hours, the WT strain (M =1.18, SD = 0.09), showed a significantly greater growth compared to the Δ*PA1759-60* mutant (M = 0.76, SD = 0.04), $t(4) = 6.90$, $p < 0.001$.

These results demonstrate that the Δ*PA1759-60* mutant exhibits reduced growth under aerobic conditions compared to the WT, which is consistent with previous findings from the Mah lab that reported similar observations.

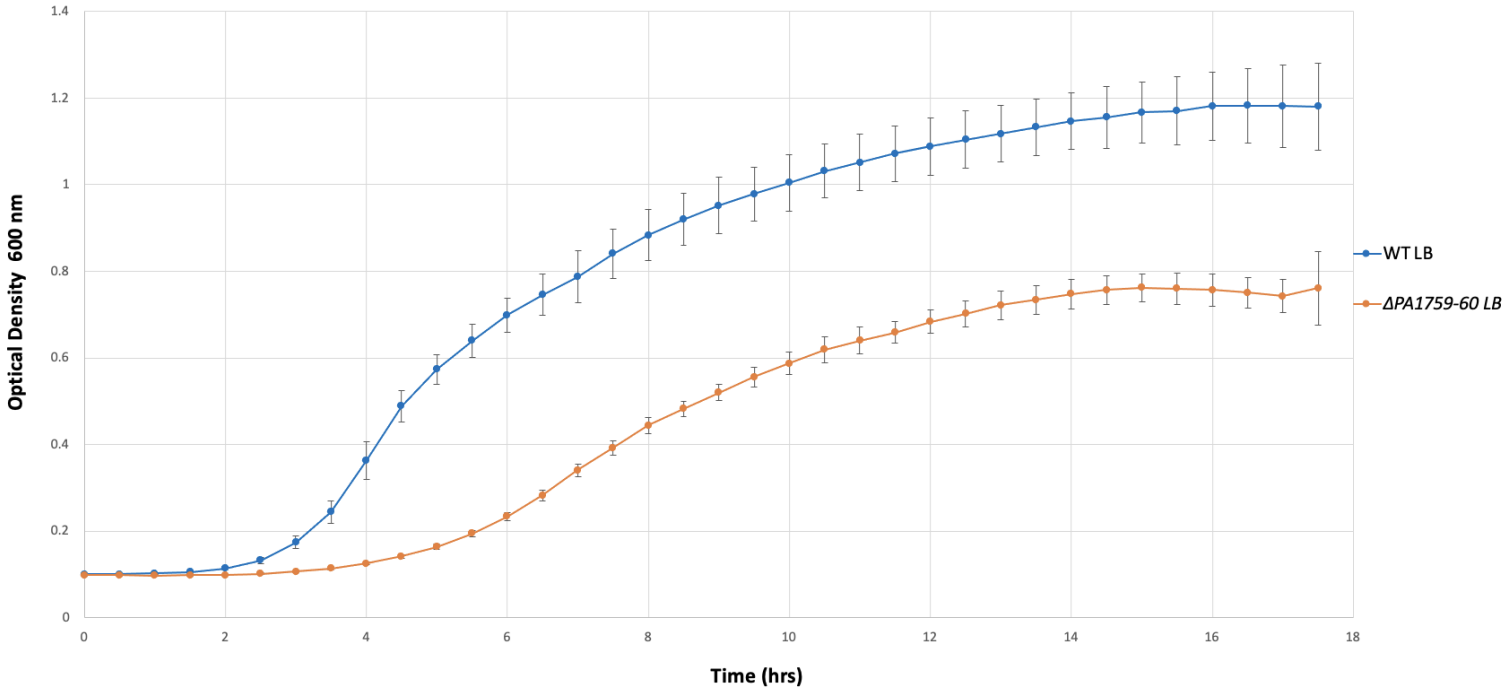

Figure 4: Aerobic growth curve of PA14 WT, and double deletion mutant Δ*PA1759-60* in LB medium. The growth curves depict the optical density (OD) at 600 nm over a duration of 18hrs at 37°C. Error bars indicates standard error (SE), n = 3

3.2 Aerobic Biofilm Formation - Crystal Violet Assay

The aerobic biofilm test was done to test the Δ*PA1759-60* ability to form biofilms in aerobic conditions using a well-established microtiter dish protocol with crystal violet staining. This is an effective and standard method for studying and analyzing the early phases of biofilm formation due to its ability to provide clear and reliable results (O'Toole, 2011).

The aerobic biofilm assay results showed that both WT and Δ*PA1759-60* can form biofilms (Figure 5), with WT having a stronger biofilm than the mutant indicated by a prominent purple ring at the air-liquid interface. In contrast, the negative control, Δ*flgK*, did not form a biofilm at the air-liquid interface. It is well-documented that this mutant does not form a biofilm under aerobic conditions due to a mutation in its flagellar hook, preventing its ability to swim to the surface of the wells (O'Toole and Kolter, 1998). These qualitative results suggest that while both the Δ*PA1759-60* mutant and the WT can form a biofilm, the mutant forms a moderate biofilm, whereas the WT forms a strong biofilm (Singh et al., 2019).

The images of the biofilms formed by the different strains were used as a qualitative assessment, which was then followed by quantification to provide a measurable comparison of biofilm formation. To quantify the biofilm formation, the absorbance readings were taken at 595 nm for the WT, Δ*PA1759-60*, and Δ*flgK* strains and these were compared to the blank control. In Figure 6, the quantification of the 24 hours of the aerobic biofilm formation supports the previous observations, where the WT displayed the strongest level of biofilm formation, the Δ*PA1759-60* showed a moderate level of biofilm formation. The mutant Δ*flgK* exhibited the weakest level of biofilm formation in comparison to WT and Δ*PA1759-60* mutant where the

absorbance values at all time points were above the absorbance values measured for the blank control.

To statistically analyze the differences in OD595 absorbance with the strains at 24 hours, a one-way ANOVA was performed. The ANOVA results indicated significant differences among the strains at all time points: 24 hours ($F(2, 6) = 9.50$, $p < 0.05$). Following the ANOVA, the post-hoc Tukey's HSD test was conducted to identify specific pairwise differences. The post-hoc Tukey's HSD test clarified which specific pairs of strains had significant differences in biofilm formation at each time point. The results revealed that at 24 hours WT and Δ*PA1759-60* were significantly different from each other, as well as WT and Δ*flgK*, while Δ*flgK* and Δ*PA1759-60*, were not significantly different (Figure 6).

By focusing on the trend of results in Figure 6, a consistent pattern across the different time points can be observed: WT exhibited the highest biofilm formation, Δ*PA1759-60* showed a moderate biofilm formation relative to WT, and Δ*flgK* showed the weakest biofilm formation in comparison to all strains.

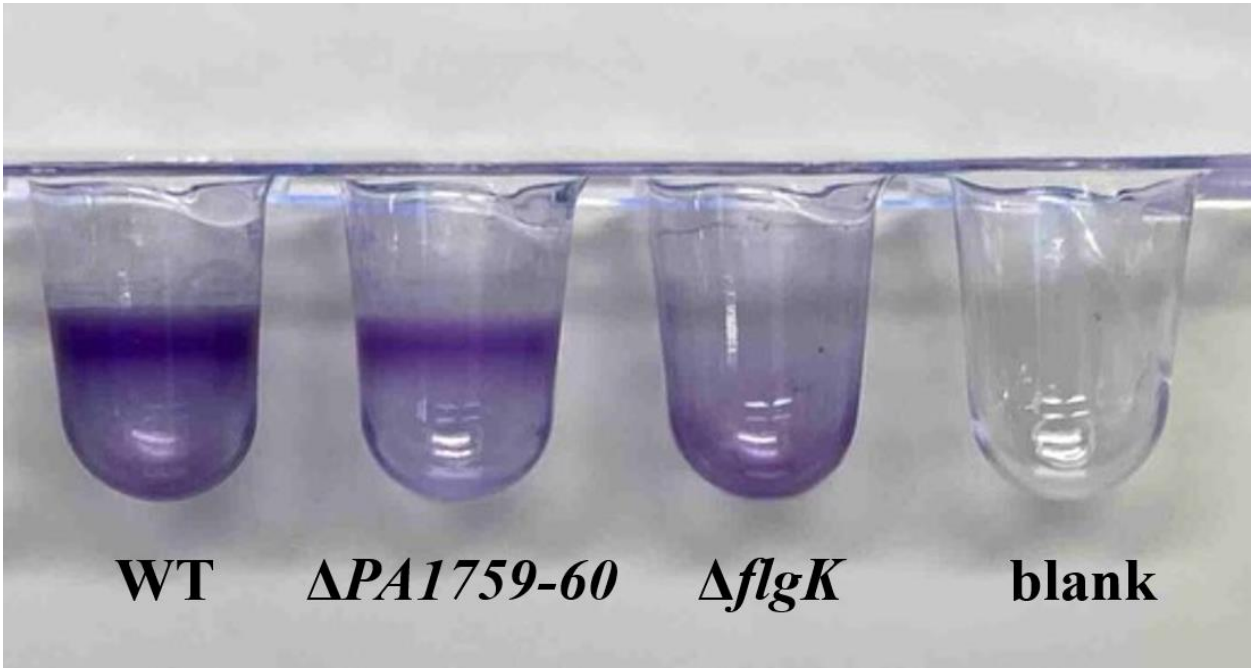

Figure 5: Side view of a 96-microtiter plate of aerobic biofilm formation of PA14 WT, Δ*PA1759-60* and Δ*flgK* in M63 over the period of 24hrs. A blank control (containing only M63 medium without bacteria) followed the same experimental procedures as the other strains. Purple ring indicates on the wells indicates biofilm formation. n = 3

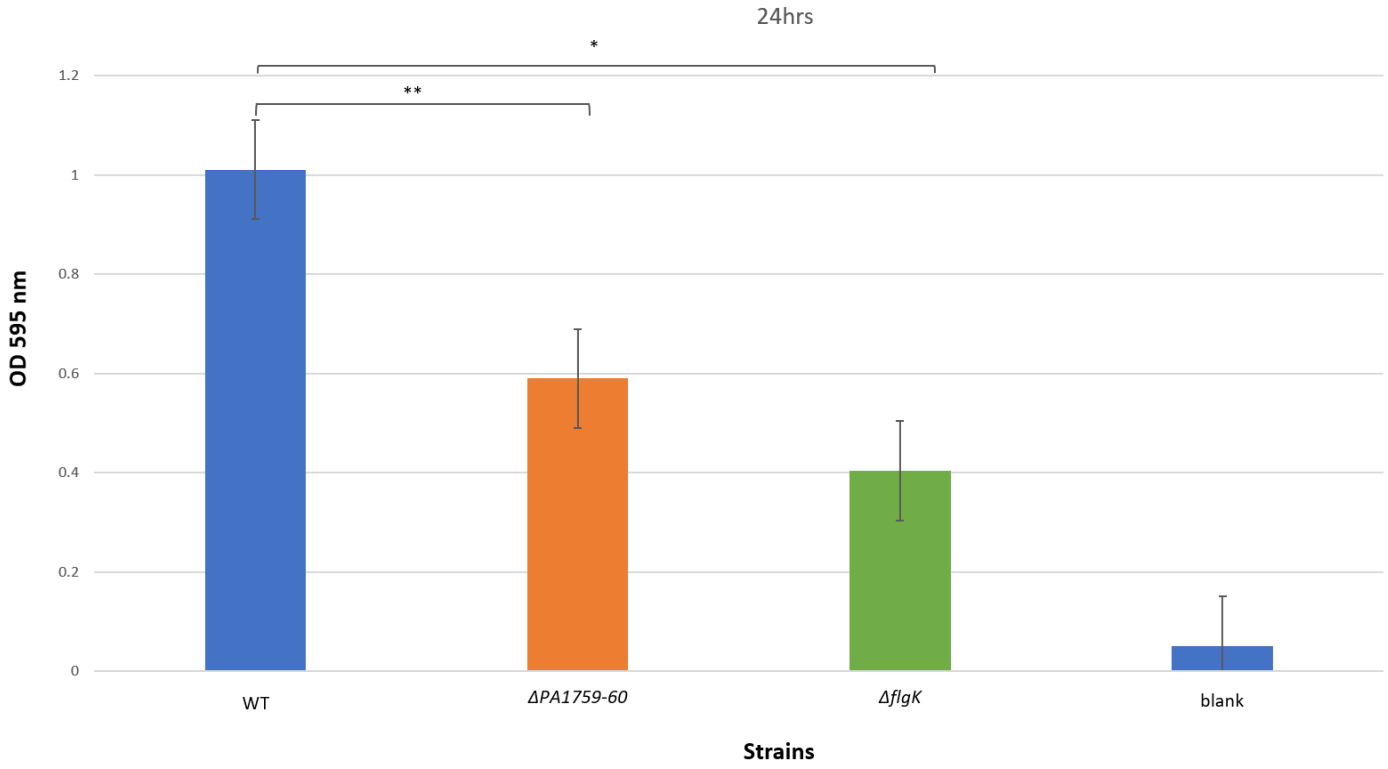

Figure 6: Quantification of 24hrs aerobic biofilm formation of PA14 WT, Δ*PA1759-60*, Δ*flgK*, and a blank control (containing only M63 medium without bacteria) followed the same experimental procedures as the other strains. Crystal violet-stained biofilm was resuspended in 30% acetic acid and OD595 was measured. A one-way ANOVA indicated significant differences among strains at 24hrs ($F(2, 6) = 9.50$, $p < 0.05$), and post-hoc Tukey's HSD test showed WT and Δ*PA1759-60* were significantly different represented by ** ($p < 0.01$). While WT and Δ*flgK*, were significantly different represented by * ($p < 0.05$) and Δ*flgK* and Δ*PA1759-60* were not significantly different. Error bars indicates standard error (SE), n = 3

3.3 Anaerobic Growth Assay

An anaerobic growth assay was conducted to assess the phenotype of the Δ*PA1759-60* mutant under anaerobic conditions. This was necessary to assess whether the growth characteristics observed under aerobic conditions would be consistent when oxygen was absent, thereby providing an understanding of the mutant's ability to grow in different environments. The results (Figure 7) showed that the WT exhibited a strong growth under anaerobic conditions in LBN medium. In contrast, the mutant Δ*PA1759-60* displayed diminished growth compared to WT, failing to achieve the anticipated OD comparable to WT.

To provide a quantitative analysis of the growth curves and allow for a better comparison of the differences in growth, the percentage difference in optical density was calculated between WT and the Δ*PA1759-60* mutant strain at the 10 hour point and at the 17.5 hour point (Figure 7). At the 10 hour point the percentage difference for the anaerobic growth was that the mutant Δ*PA1759-60* showed a 41.6% lower OD compared to WT and at the 17.5 hour point the mutant showed a 39.6% lower OD compared to the WT.

Additionally, a statistical analysis using a two-tailed t-test was performed to compare the difference in growth of the WT and the Δ*PA1759-60* mutant at the 10 hour and 17.5 hour points. The test assumed equal variances and independent samples for both strains.

At the 10 hours, the WT strain ($M = 0.47$, $SD = 0.07$) has a significantly higher growth compared to the Δ*PA1759-60* mutant ($M = 0.27$, $SD = 0.03$), $t(4) = 4.32$, $p < 0.05$. Similarly at 17.5 hours, the WT strain ($M = 0.58$, $SD = 0.09$), showed a significantly greater growth compared to the Δ*PA1759-60* mutant ($M = 0.35$, $SD = 0.05$), $t(4) = 3.77$, $p < 0.05$.

These results indicate that, in comparison to the WT, the mutant Δ*PA1759-60* shows a deficiency of growth phenotype in anaerobic circumstances.

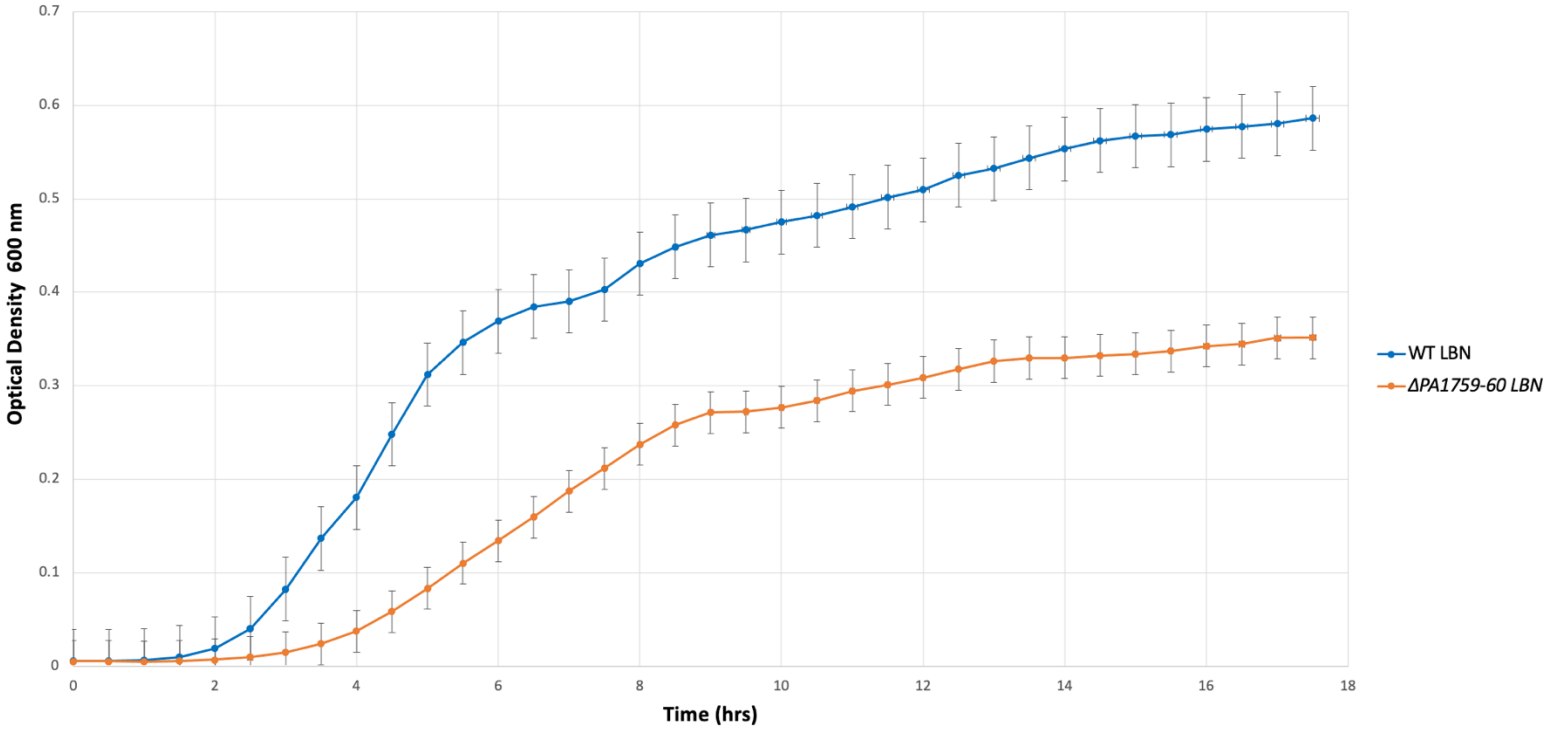

Figure 7: Anaerobic growth curve of PA14 WT, and double deletion mutant Δ*PA1759-60* in LBN medium. The growth curves depict the optical density (OD) at 600 nm over a duration of 18hrs at 37°C. Error bars indicates standard error (SE), n = 3

3.4 Anaerobic Biofilm Formation – Crystal Violet Assay

Following the analysis of the biofilm formation phenotype of the *ΔPA1759-60* mutant under aerobic conditions, it was important to further investigate its phenotype under anaerobic conditions. Considering the differences in aerobic and anaerobic environments, it was uncertain whether the results for biofilm formation in aerobic conditions would be the same in anaerobic conditions. A crystal violet assay under anaerobic conditions was required to properly understand the different phenotype of *ΔPA1759-60* biofilm formation in the absence of oxygen.

Results obtained showed that, in the absence of oxygen, biofilm formation occurred at the bottom of the wells rather than at the air-liquid interface (Figure 9). At the 24 hour mark, the WT strain formed a strong biofilm, evident from the deep purple stain in the well. The Δ*PA1759-60* mutant exhibited a severe biofilm deficiency phenotype, indicated by the faint purple colour at the bottom of the well (Figure 8 and Figure 9). In contrast, the Δ*flgK*, displayed a moderate biofilm formation under anaerobic conditions in comparison to the Δ*PA1759-60* mutant, with a moderate amount of the purple stain accumulating in the well. However, the biofilm formation of Δ*flgK*, was still weaker than that of the WT based on the intensity of the purple stain in the wells.

The Δ*flgK* mutant is commonly used as a negative control for aerobic biofilm formation. However, under anaerobic conditions this mutant formed a biofilm despite lacking a flagellum and being unable to swim to the surface of the wells. In anaerobic conditions, cells don’t need to swim to the air-liquid interface to form biofilms, with the influence of gravity, cells can accumulate at the bottom of the wells and form biofilms. This was observed with the Δ*flgK*

mutant, indicating that it cannot be considered a negative control for anaerobic biofilm formation.

At the 48 hour mark, WT still showed a strong biofilm formation, seen by the deep purple stain, while Δ*flgK* also showed a more moderate biofilm formation though less than the WT. In contrast, the Δ*PA1759-60* continued to show a weak biofilm phenotype in comparison to the other strains as seen by the faint purple stain in the well (Figure 9). At the 72 hours mark, the same pattern is displayed where the WT continued to show the strongest biofilm formation, Δ*flgK* continued to show a moderate level of biofilm formation and Δ*PA1759-60* continued to show the weakest biofilm formation (Figure 9). These qualitative results indicate that WT can form biofilms under anaerobic conditions, while Δ*PA1759-60* exhibits a significant deficiency in biofilm formation. The qualitative results demonstrating that WT and Δ*PA1759-60* are significantly different are further supported by the quantification results.

To quantify the biofilm formation, the absorbance readings were taken at 595 nm for the WT, Δ*PA1759-60*, and Δ*flgK* strains and these were compared to the blank control, which consisted of wells containing only M63N medium without bacteria that underwent the same experimental steps as the other strains. In Figure 11, the quantification of the 24, 48 and 72 hours of the anaerobic biofilm formation supports the previous observations, where the WT displayed the strongest level of biofilm formation in all the time points and the Δ*flgK* showed a moderate level of biofilm formation. Δ*PA1759-60* exhibited the weakest level of biofilm formation where the absorbance values at all time points were minimally above the absorbance values measured for the blank control.

To statistically analyze the differences in OD595 absorbance with the strains at 24, 48, and 72 hours, a one-way ANOVA was performed. The ANOVA results indicated significant

differences among the strains at all time points: 24 hours ($F(2, 6) = 5.17$, $p < 0.05$), 48 hours ($F(2, 6) = 45.7$, $p < 0.05$), and 72 hours ($F(2, 6) = 10.48$, $p < 0.05$). Following the ANOVA, the post-hoc Tukey's HSD test was conducted to identify specific pairwise differences.

The post-hoc Tukey's HSD test clarified which specific pairs of strains had significant differences in biofilm formation at each time point. The results revealed that at 24 hours only WT and Δ*PA1759-60* were significantly different from each other, while WT and Δ*flgK*, as well as Δ*flgK* and Δ*PA1759-60*, were not significantly different (Figure 10 and Figure 11). At 48 hours, all strains (WT, Δ*PA1759-60*, and Δ*flgK*) were significantly different from each other (Figure 11). At 72 hours, only WT and Δ*PA1759-60* were significantly different (Figure 11). By focusing on the trend of results in Figure 11, a consistent pattern across the different time points can be observed: WT exhibited the highest biofilm formation, Δ*flgK* showed a moderate biofilm formation relative to WT, and Δ*PA1759-60* showed the lowest biofilm formation among all strains.

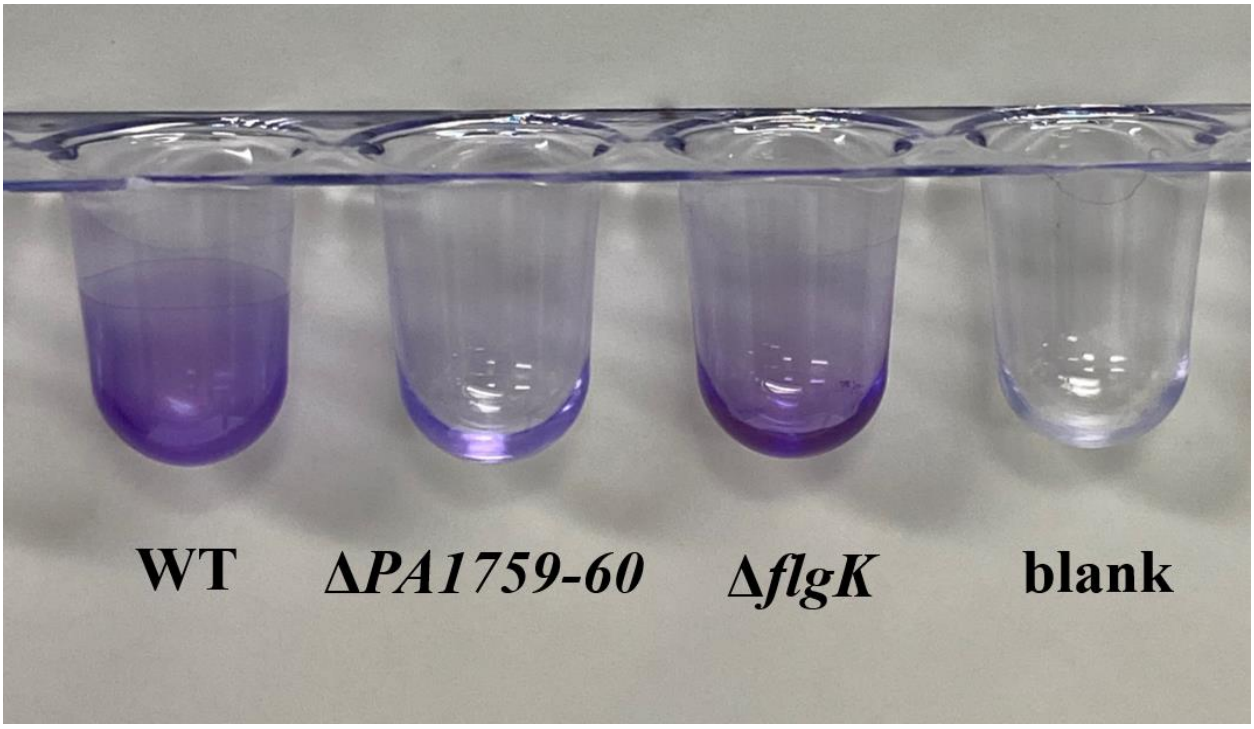

Figure 8: Side view of a 96-microtiter plate of anaerobic biofilm formation of PA14 WT, Δ*PA1759-60* and Δ*flgK* in M63N over the period of 24hrs. A blank control (containing only M63N medium without bacteria) followed the same experimental procedures as the other strains. Purple staining at the bottom of the wells indicates biofilm formation. n = 3

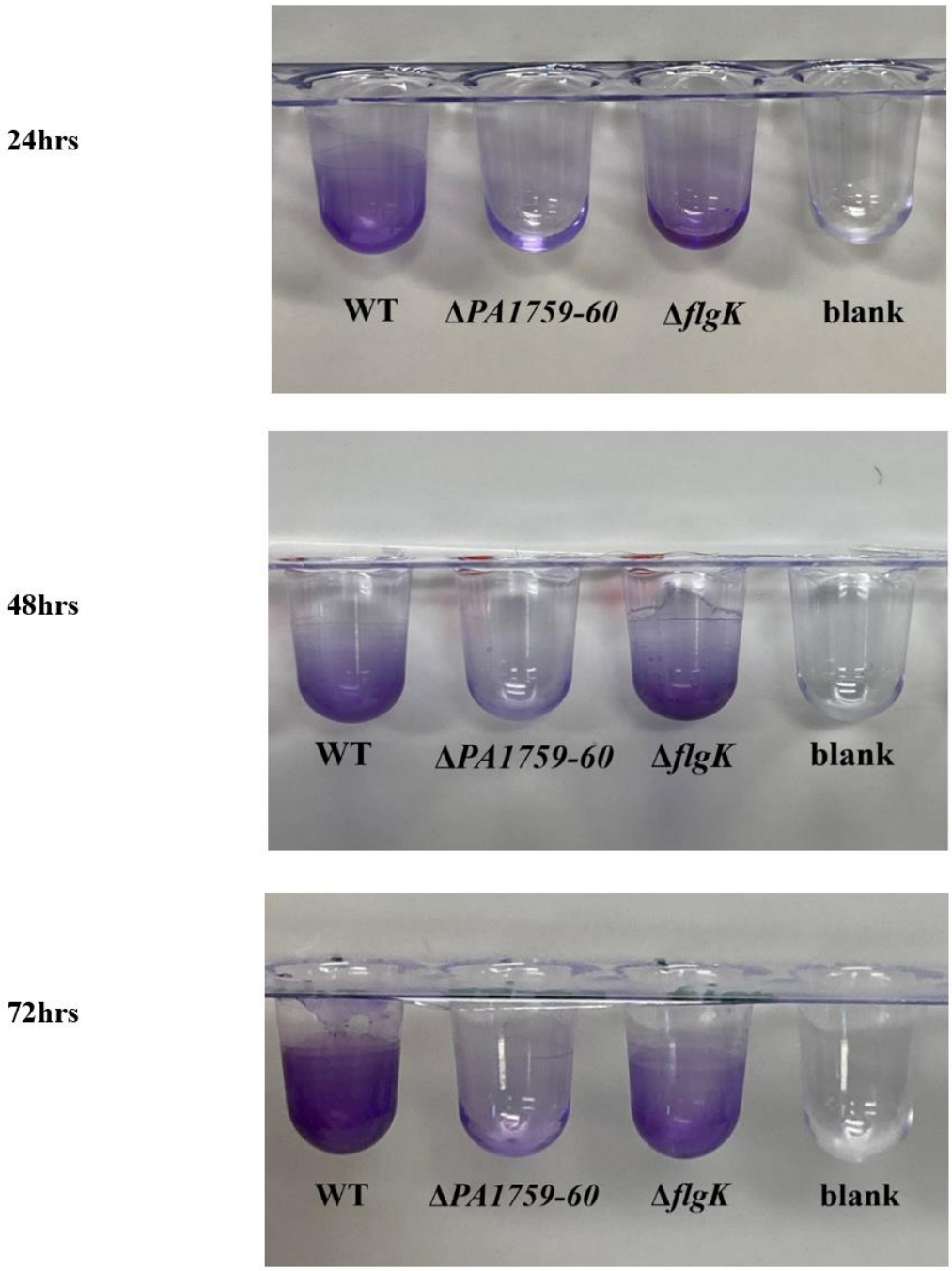

Figure 9: Side view of a 96-microtiter plate of anaerobic biofilm formation at different time points 24, 48, 72hrs of PA14 WT, Δ*PA1759-60* and Δ*flgK* in M63N. A blank control (containing only M63N medium without bacteria) followed the same experimental procedures as the other strains. Purple staining at the bottom of the wells indicates biofilm formation. n = 3

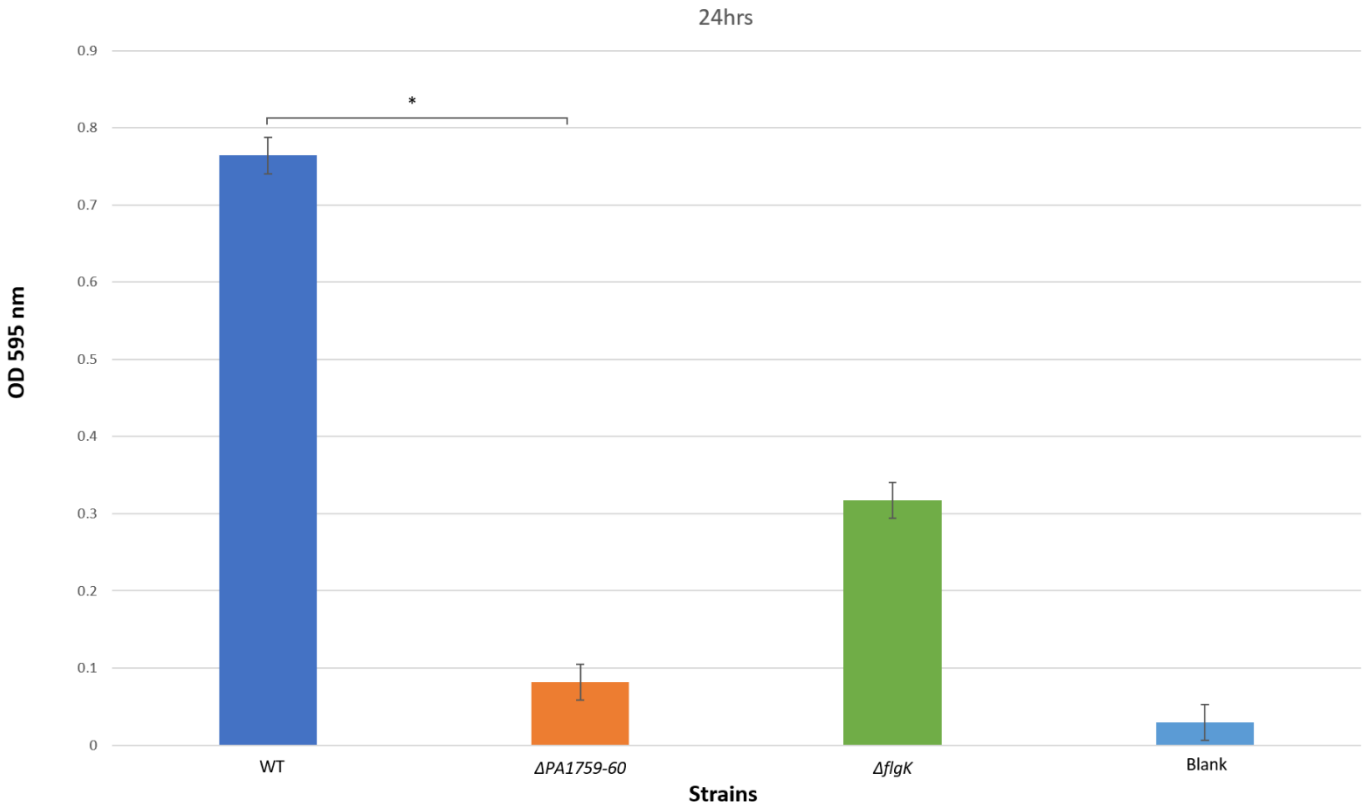

Figure 10: Quantification of 24hrs anaerobic biofilm formation of PA14 WT, Δ*PA1759-60*, Δ*flgK*, and a blank control (containing only M63N medium without bacteria) followed the same experimental procedures as the other strains. Crystal violet-stained biofilm was resuspended in 30% acetic acid and OD595 was measured. A one-way ANOVA indicated significant differences among strains at 24hrs ($F(2, 6) = 5.17$, $p < 0.05$), and post-hoc Tukey's HSD test showed WT and Δ*PA1759-60* were significantly different represented by * ($p < 0.05$). While WT and Δ*flgK*, and Δ*flgK* and Δ*PA1759-60* were not significantly different. Error bars indicates standard error (SE), n = 3

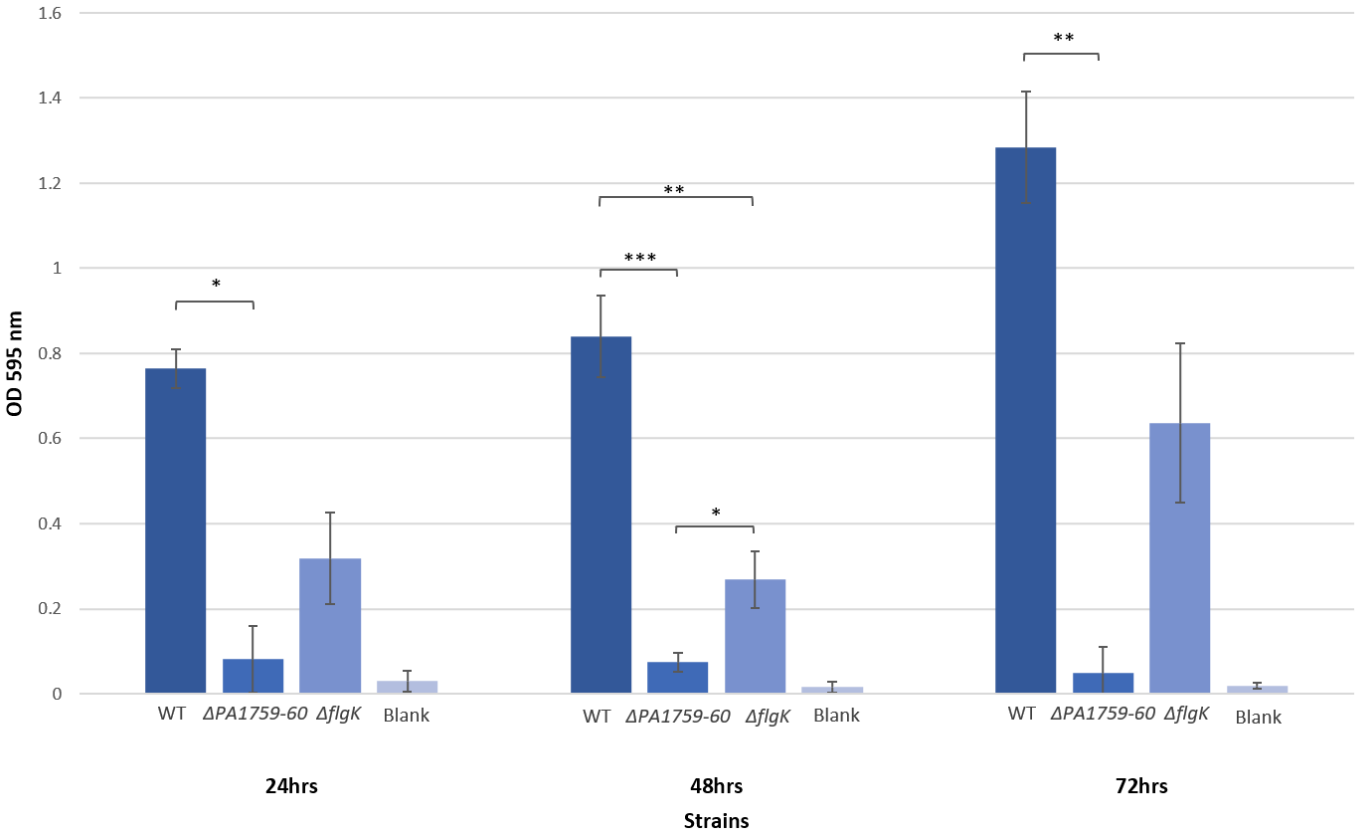

Figure 11: Quantification of 24hrs, 48hrs and 72hrs anaerobic biofilm formation of PA14 WT, Δ*PA1759-60*, Δ*flgK* and a blank control (containing only M63N medium without bacteria) followed the same experimental procedures as the other strains. The data at 24hrs, first shown in Figure 10, is reproduced here to facilitate comparison. Crystal violet-stained biofilm was resuspended in 30% acetic acid, and OD595 was measured. A one-way ANOVA revealed significant differences among strains at all time points (24hrs: $F(2, 6) = 5.17$, $p < 0.05$; 48hrs: $F(2, 6) = 45.7$, $p < 0.05$; 72hrs: $F(2, 6) = 10.48$, $p < 0.05$), and a post-hoc Tukey's HSD test indicated significant pairwise differences: at 24hrs, the pair consisting of WT and Δ*PA1759-60* was significantly different, represented by * ($p < 0.05$). At 48hrs, all strains were significantly different, represented by * ($p < 0.05$), ** ($p < 0.01$), *** ($p < 0.001$). At 72hrs, WT and Δ*PA1759-60* were significantly different, represented by ** ($p < 0.01$). Error bars indicates standard error (SE), n = 3

4.0 Discussion

The emergence of antibiotic resistance, particularly in pathogens like PA, poses a significant public health threat due to the bacterium's ability to form biofilms that protect them from conventional antibiotic treatments (Dadgostar, 2019; Murray et al., 2022). This study aimed to investigate the ability of the mutant Δ*PA1759-60* to grow and form biofilms under anaerobic conditions. The findings provide significant insights into the functional role of *PA1759-60'*s phenotype, particularly under the anaerobic conditions that may be seen in certain chronic, human infections, such as those found in CF lungs (Thornton and Surette, 2021).

A former lab technician, Li Zhang, constructed and conducted the initial analysis of the *PA1759-60* deletion mutant. Zhang's antibiotic resistance assay suggested that these genes might play a significant role in contributing to PA biofilm antibiotic resistance. However, my research has shown that this is unlikely, as I have demonstrated that the deletion mutant exhibits significant defects in both growth and biofilm formation.

The data demonstrated that the Δ*PA1759-60* mutant grew less effectively and formed significantly less biofilm than the WT strain. Specifically, the OD595 measurements indicated a clear difference in biofilm formation, with the *ΔPA1759-60* mutant showing lower values across all time points. These findings suggest that the *PA1759-60* gene may play a role in both bacterial growth and biofilm formation in anaerobic environments.

4.1 Growth Deficiency of Δ*PA1759-60* Under Aerobic and Anaerobic Conditions

The results of this study demonstrates that the Δ*PA1759-60* mutant exhibits significant growth deficiencies compared to the WT strain under both aerobic and anaerobic conditions. However, no direct comparison of growth was made between the two conditions.

In agreement with this observation, when considering the percentage difference in growth between the WT and the Δ*PA1759-60* mutant at specific timepoints, similar patterns were observed under both conditions. Under aerobic conditions, the Δ*PA1759-60* mutant showed a 41.3% decrease in OD at the 10 hour point, and at 17.5 hours, the difference decreased to 35.5%. A similar trend was seen under anaerobic conditions, where the Δ*PA1759-60* mutant exhibited a 41.6% decrease in OD at the 10 hour point, and at 17.5 hours, the difference decreased to 39.6%. While more analysis is needed to understand the underlying factors, the percentage differences are similar between the two strains and conditions.

Overall, these results suggest that the Δ*PA1759-60* mutant grows more slowly than the WT in the early stages of growth, however, further analysis and a longer time course for the growth experiments are needed to fully understand the significance of these differences across the different growth phases for each of these strains. For instance, the small but statistically significant changes in OD during both aerobic and anaerobic growth curves could suggest that, while Δ*PA1759-60* mutant strain grows more slowly than the WT in the initial stages of growth, it may still reach a similar stationary phase at a slower rate.

These TRs are predicted to be functionally redundant, as both must be deleted in order to observe a phenotype, suggesting that they may have overlapping target genes. Their impact on

growth indicates that some of these target genes are likely involved in growth regulation or metabolism. Further investigation into these gene targets could clarify how *PA1759-60* influences growth in PA.

4.2 Weak Biofilm Formation in Δ*PA1759-60* Mutant

The biofilm assays revealed that the Δ*PA1759-60* mutant exhibits a weaker biofilm formation under both aerobic and anaerobic conditions in comparison to the WT. Although both the WT and Δ*PA1759-60* strains formed biofilms aerobically, quantification revealed a reduced in biofilm formation by the mutant, with the differences being statistically significant. Under anaerobic conditions, the Δ*PA1759-60* mutant displayed an even weaker biofilm formation compared to WT. The deficiency in biofilm formation in both aerobic and anaerobic environments demonstrates that the *PA1759-60* gene has an impact on biofilm formation**,** regardless of the environment's oxygen conditions.

Since there is a growth defect under both aerobic and anaerobic conditions, it is possible that this explains the impact on biofilm formation. However, without further experiments, we cannot confirm this. Additional studies are needed to determine whether the growth defect directly influences biofilm formation or if other factors are involved.

4.3 Significance and Implications

The observed deficiencies in growth and biofilm formation in the Δ*PA1759-60* mutant suggest that the *PA1759-60* genes are involved in growth and biofilm development, however, a question is raised on whether the influence of these genes on biofilm formation is a direct effect or if its due to Δ*PA1759-60*'s growth deficiency, or whether it is a combination of both. Since both growth and biofilm formation are processes that are intertwined, it is difficult to determine if the phenotype observed in the biofilm formation assay is specifically from a disruption in biofilm regulation pathways, or if it is from the reduced cellular density observed in the growth assay.

Due to the fact that growth and biofilm formation are intertwined, it is challenging to understand and determine the phenotype of the Δ*PA1759-60* under both aerobic and anaerobic conditions. To address this challenge, experiments can be conducted to delve more deeply into the mutant's phenotype in growth and biofilm formation. As mentioned, conducting a growth assay over a prolonged period of time will further determine the mutant's growth phenotype. Additionally, performing a chemostat experiment would also allow the observation of a steady growth of planktonic cells in a more controlled environment. A comparison between the phenotype of the mutant and the WT might yield further insights. This approach would also allow for the analysis of cell density and metabolic activities in both strains (Miller et al., 2013).

For biofilm formation, a flow cell system can be used to assess biofilm formation as it allows for continuous observation of biofilm formation over time, using this type of experiment would allow us to observe biofilm formation in a controlled environment, where the bacteria is

exposed to a constant flow of nutrients and oxygen levels while simulating realistic conditions. As previously shown in Figure 1, there are important stages that cells need to go through to form a biofilm, such as attaching to a surface, formation of a microcolony and then maturation into a macrocolony. By using a flow cell system, this would be an effective method to study whether the mutant is deficient at any of these stages, and this would give more insight into the mutant's ability to form biofilms (Weiss Nielsen et al., 2011).

Finally, to further address this limitation, it would be useful to carry out gene expression analysis, such as RNA-sequencing. This approach would involve comparing the genes expressed in the WT to those expressed in the mutant to identify differentially expressed genes. By analyzing these differences, it would be possible to identify potential target genes of *PA1759-60.* This list of genes could then be examined to determine which ones may be contributing to the slower growth rate of the mutant and which genes might be affecting biofilm formation (Deng et al., 2023).

A limitation of this study is the reliance on OD measurements without performing plate counts to determine colony-forming units (CFUs). While OD readings were done for the growth assays and biofilm assays to provide a relative measure of bacterial density, they do not distinguish between live and dead cells in a culture. As a result, the presence of dead cells in the culture at the time of measurement could have inflated the OD results and potentially affected the interpretation of the growth and biofilm formation results. In order to address this limitation, it would be ideal for future experiments to incorporate CFU counts to provide more accurate assessments of viable cell density and strengthen the results of both assays.

5.0 Future Directions and Conclusion

As previously mentioned, the decision to analyze the TRs PA1759 and PA1760 came from the identification of the PA1759 tn-mutant from a screen of tn-insertion mutants of all predicted TRs in the PA14 genome. Of the thirteen TRs identified in the screen, it is the only one in which a deletion mutant has been constructed and characterized. Thus, a future research direction could be to analyze the other twelve TRs in a similar fashion.

Additionally, future research should focus on further investigating the roles of the genes PA1759 and PA1760 and their encoded proteins. While these genes have been identified in a screen for antibiotic resistance, the work presented in this thesis suggests that they are more likely to influence growth and biofilm formation under both aerobic and anaerobic conditions rather than directly regulating antimicrobial resistance mechanisms. Given that biofilm formation is an essential step towards the persistence of a chronic bacterial infection, these genes could be considered as being indirectly involved in biofilm-mediated antibiotic resistance.

Once the roles of PA1759 and PA1760 in growth and biofilm formation have been fully characterized, future research should also focus on *in vivo* models, as this research primarily explored biofilm formation under controlled aerobic and anaerobic conditions *in vitro*, which do not fully replicate the complex and dynamic environments of clinical infections. Factors such as nutrient availability, host immune responses, and the presence of other microbial species were not addressed, limiting this study's ability to capture the complete range of conditions encountered by PA.

In conclusion, this study has investigated the role of Δ*PA1759-60* in growth and biofilm formation in both aerobic and anaerobic settings. The significant deficiencies observed in the *ΔPA1759-60* mutant highlights the potential of targeting *PA1759-60* as a strategy to disrupt growth and biofilm formation, leading to the possible development of treatments to reduce biofilm-associated illnesses.

References

Acosta N, Waddell B, Heirali A, Somayaji R, Surette MG, Workentine ML, Rabin HR, Parkins MD. 2020. Cystic fibrosis Patients infected with epidemic *Pseudomonas aeruginosa* strains have unique microbial communities. Front Cell Infect Microbiol 10.

Alotaibi GF. 2021. Factors influencing bacterial biofilm formation and development. Am J Biomed Sci Res 12:617–626.

Altschul SF, Gish W, Miller W, Myers EW, Lipman DJ. 1990. Basic local alignment search tool J. Mol. Biol 215:403–410

Beaudoin T, Zhang L, Hinz AJ, Parr CJ, Mah TF. 2012. The biofilm-specific antibiotic resistance gene *ndvB* is important for expression of ethanol oxidation genes in *Pseudomonas aeruginosa* biofilms. J Bacteriol 194:3128–3136.

Bengtsson-Palme J, Kristiansson E, Larsson DGJ. 2018. Environmental factors influencing the development and spread of antibiotic resistance. FEMS Microbiol Rev 42

Berlanga M, Guerrero R. 2016. Living together in biofilms: The microbial cell factory and its biotechnological implications. Microb Cell Fact 15.

Bhagirath AY, Li Y, Somayajula D, Dadashi M, Badr S, Duan K. 2016. Cystic fibrosis lung environment and *Pseudomonas aeruginosa* infection. BMC Pulm Med 16:174.

Bodey GP, Bolivar R, Fainstein V, Jadeja L. 1983. Infections caused by *Pseudomonas aeruginosa*. Rev Infect Dis 5:279–313.

Bulitta JB, Ly NS, Landersdorfer CB, Wanigaratne NA, Velkov T, Yadav R, Oliver A, Martin L, Shin BS, Forrest A, Tsuji BT. 2015. Two mechanisms of killing of *Pseudomonas aeruginosa* by Tobramycin assessed at multiple inocula via mechanism-based modeling. AAC 59:2315–2327.

Conrad Jacinta C, Gibiansky Maxsim L, Jin F, Gordon Vernita D, Motto Dominick A, Mathewson Margie A, Stopka Wiktor G, Zelasko Daria C, Shrout Joshua D, Wong Gerard CL. 2011. Flagella and Pili-mediated near-surface single-cell motility mechanisms in *P. aeruginosa*. Biophys J 100:1608–1616.

Centers for Disease Control and Prevention. 2019. Antibiotic Resistance Threats in the United States, 2019. Atlanta, Georgia.

Chandler CE, Horspool AM, Hill PJ, Wozniak DJ, Schertzer JW, Rasko DA, Ernsta RK. 2019. Genomic and phenotypic diversity among ten laboratory isolates of *Pseudomonas aeruginosa* PAO1. J Bacteriol 201:00595-18.

Codjo EA, Edmond SA, Hermann H, Romain GK. 2024. On the use of post-hoc tests in environmental and biological sciences: A critical review. Heliyon 10:e25131–e25131.

Dadgostar P. 2019. Antimicrobial resistance: implications and costs. Infect Drug Resist 12:3903–3910

Danot O. 2001. A complex signaling module governs the activity of MalT, the prototype of an emerging transactivator family. Proc Natl Acad Sci 98:435–440.

Davies J. 2002. *Pseudomonas aeruginosa* in Cystic fibrosis: pathogenesis and persistence. Paediatr Respir Rev 3:128–134.

Deng W, Zhou C, Qin J, Jiang Y, Li D, Tang X, Luo J, Kong J, Wang K. 2023. Molecular mechanisms of DNAse inhibition of early biofilm formation *Pseudomonas aeruginosa* or *Staphylococcus aureus*: A transcriptome analysis. Biofilm 7.

Donlan RM. 2002. Biofilms: Microbial Life on Surfaces. Emerg Infect Dis 8:881–890.

Fajardo A, Martínez-Martín N, Mercadillo M, Galán JC, Ghysels B, Matthijs S, Cornelis P, Wiehlmann L, Tümmler B, Baquero F, Martínez JL. 2008. The neglected intrinsic resistome of bacterial pathogens. PLoS One 3:e1619.

Ferrer-Espada R, Shahrour H, Pitts B, Stewart PS, Sánchez-Gómez S, Martínez-de-Tejada G. 2019. A permeability-increasing drug synergizes with bacterial efflux pump inhibitors and restores susceptibility to antibiotics in multi-drug resistant *Pseudomonas aeruginosa* strains. Scie Rep 9:3452.

Fischer AJ, Singh SB, LaMarche MM, Maakestad LJ, Kienenberger ZE, Peña TA, Stoltz DA, Limoli DH. 2021. Sustained coinfections with *Staphylococcus aureus* and *Pseudomonas aeruginosa* in Cystic fibrosis. Am J Resp Crit Care Med 203.

Furiga A, Lajoie B, El Hage S, Baziard G, Roques C. 2015. Impairment of *Pseudomonas aeruginosa* Biofilm resistance to antibiotics by combining the drugs with a new Quorum-Sensing inhibitor. Antimicrob Agents and Chemother 60:1676–1686.

Grace A, Sahu R, Owen DR, Dennis VA. 2022. *Pseudomonas aeruginosa* reference strains PAO1 and PA14: A genomic, phenotypic, and therapeutic review. Front Microbiol 13:1023523

Grooters KE, Ku JC, Richter DM, Kirnock MJ, Minor A, Li P, Kim A, Sawyer R, Li Y. 2024. Strategies for combating antibiotic resistance in bacterial biofilms. Front Cell Infect Microbiol 14.

Hall CW, Mah TF. 2017. Molecular mechanisms of biofilm-based antibiotic resistance and tolerance in pathogenic bacteria. FEMS Microbiol Rev 41:276-301.

Harrison EM, Carter MEK, Luck S, Ou H-Y ., He X, Deng Z, O'Callaghan C, Kadioglu A, Rajakumar K. 2010. Pathogenicity islands PAPI-1 and PAPI-2 contribute individually and synergistically to the virulence of *Pseudomonas aeruginosa* strain PA14. Infect Immun 78:1437–1446.

Hobley L, Harkins C, MacPhee CE, Stanley-Wall NR. 2015. Giving structure to the biofilm matrix: An overview of individual strategies and emerging common themes. FEMS Microbiol Rev 39:649–669.

Hotterbeekx A, Kumar-Singh S, Goossens H, Malhotra-Kumar S. 2017. *In vivo* and *In vitro* interactions between *Pseudomonas aeruginosa and Staphylococcus spp*. Front Cell Infect Microbiol 7:106.

Jefferson KK. 2004 .What drives bacteria to produce a biofilm? FEMS Microbiol Lett 236:163–173.

Kaushik KS, Stolhandske J, Shindell O, Smyth HD, Gordon VD. 2016.Tobramycin and bicarbonate synergise to kill planktonic *Pseudomonas aeruginosa* but antagonise to promote biofilm survival. Npj Biofilms and Microbiomes 2

Krasovec M, Hoshino M, Zheng M, Lipinska AP, Coelho SM. 2023. Low spontaneous mutation rate in complex multicellular Eukaryotes with a haploid-diploid life cycle. Mol Biol Evol 40.

Krause KM, Serio AW, Kane TR, Connolly LE. 2016. Aminoglycosides: an overview. Cold Spring Harbor Perspectives in Medicine 6:a027029.

Lee DG, Urbach JM, Wu G, Liberati NT, Feinbaum RL, Miyata S, Diggins LT, He J, Saucier M, Déziel E, Friedman L, Li L, Grills G, Montgomery K, Kucherlapati R, Rahme LG, Ausubel FM. 2006. Genomic analysis reveals that *Pseudomonas aeruginosa* virulence is combinatorial. Genome Biol 7.

Liao J, Sauer K. 2012. The MerR-Like transcriptional regulator BrlR contributes to *Pseudomonas aeruginosa* biofilm tolerance. J Bacter 194:4823–4836.

Mah TF, Pitts B, Pellock B, Walker GC, Stewart PS, O'Toole GA. 2003. A genetic basis for *Pseudomonas aeruginosa* biofilm antibiotic resistance. Nature 426:306–310.

Mangiaterra G, Cedraro N, Vaiasicca S, Citterio B, Frangipani E, Biavasco F, Vignaroli C. 2023. Involvement of Acquired Tobramycin Resistance in the Shift to the Viable but Non-Culturable State in *Pseudomonas aeruginosa*. Int J Mol Sci 24:11618.

Martinez JL, Baquero F. 2000. Mutation frequencies and antibiotic resistance. Antimicrob Agents Chemother 44:1771–1777.

Mathee K. 2018. Forensic investigation into the origin of *Pseudomonas aeruginosa* PA14 - old but not lost. J Med Microbiol 67:1019–1021.

Maunders E, Welch M. 2017. Matrix exopolysaccharides; the sticky side of biofilm formation. FEMS Microbiol Lett 364.

Miller AW, Befort C, Kerr EO, Dunham MJ. 2013. Design and use of multiplexed chemostat arrays. J Vis Exp. 72

Murray CJL, et al. 2022. Global burden of bacterial antimicrobial resistance in 2019: a systematic analysis. The Lancet 399:629–655.

O’May CY, Reid DW, Kirov SM. 2006. Anaerobic culture conditions favor biofilm-like phenotypes in *Pseudomonas aeruginosa* isolates from patients with Cystic fibrosis. FEMS Immunol Med Microb 48:373–380.

O'Toole GA. 2011. Microtiter dish biofilm formation assay. J Vis Exp. 47

O’Toole GA, Kolter R. 1998 . Flagellar and twitching motility are necessary for *Pseudomonas aeruginosa* biofilm development. Mol Microbiol 30:295–304.

Palmer KL, Aye LM, Whiteley M. 2007 . Nutritional cues control *Pseudomonas aeruginosa* multicellular behavior in cystic fibrosis sputum. J Bacteriol 189:8079–8087.

Pang Z, Raudonis R, Glick BR, Lin TJ, Cheng Z. 2019. Antibiotic resistance in *Pseudomonas aeruginosa*: mechanisms and alternative therapeutic strategies. Biotechnol Adv 37:177–192.

Paysan-Lafosse T, Andreeva A, Blum M, Chuguransky S, Grego T, Pinto B, Salazar G, Bileschi M, Llinares-López F, Meng-Papaxanthos L, Colwell L, Grishin N, Schaeffer RD, Clementel D, Tosatto SE, Sonhammer E, Wood V, Bateman A. 2024. The Pfam protein families database: embracing AI/ML. Nucleic Acid Res.

Prestinaci F, Pezzotti P, Pantosti A. 2015. Antimicrobial resistance: a global multifaceted phenomenon. Pathog Glob Health 109:309–318.

Public Health Canada. 2024. Canadian Antimicrobial Resistance Surveillance System (CARSS) – Ottawa, ON. https://www.canada.ca/en/public-health/services/publications/drugs-health-products/canadian-antimicrobial-resistance-surveillance-system-2024-executive-summary.html#a9.

Rahme LG, Stevens EJ, Wolfort SF, Shao J, Tompkins RG, Ausubel FM. 1995. Common virulence factors for bacterial pathogenicity in plants and animals. Science 268:1899–1902.

Reece E, de Almeida Bettio PH, Renwick J. 2021. Polymicrobial interactions in the Cystic fibrosis airway microbiome impact the antimicrobial susceptibility of *Pseudomonas aeruginosa*. Antibiotics 10:827.

Reen FJ, Barret M, Fargier E, O’Muinneacháin M, O’Gara F. 2013. Molecular evolution of LysR-type transcriptional regulation in *Pseudomonas aeruginosa*. Mol Phylogenet Evol 66:1041–1049.

Reig S, Le Gouellec A, Bleves S. 2022. What Is New in the Anti–*Pseudomonas aeruginosa* clinical development pipeline since the 2017 WHO alert?. Front Cell Infect Microbiol 12.

Rudnick W, Mukhi S, Reid-Smith R, German G, Nichani A, Mulvey M. 2022. Overview of Canada’s antimicrobial resistance network (AMRNet): A data-driven one health approach to antimicrobial resistance surveillance. Canada Communicable Disease Report 48:522–528.

Sánchez-Jiménez A, Llamas MA, Francisco Javier Marcos-Torres. 2023. Transcriptional regulators controlling virulence in *Pseudomonas aeruginosa*. Int. J. Mol. Sci. 24:11895–11895.

Schroth MN, Cho JJ, Green SK, Kominos SD. 1977. Epidemiology of *Pseudomonas aeruginosa* in agricultural areas. J Med Microbiol 67:1191–1201.

Shree P, Singh CK, Sodhi KK, Surya JN, Singh DK. 2023. Biofilms: understanding the structure and contribution towards bacterial resistance in antibiotics. Medicine in Microecology 16:100084.

Singh AK, Yadav S, Chauhan BS, Nandy N, Singh R, Neogi K, Roy JK, Srikrishna S, Singh RK, Prakash P. 2019. Classification of clinical isolates of *Klebsiella pneumoniae* based on their *in vitro* biofilm forming capabilities and elucidation of the biofilm matrix chemistry with special reference to the protein content. Front Microbiol 10:669.

Solovyev V, Salamov A. 2011. Automatic annotation of microbial genomes and metagenomic sequences. In metagenomics and its applications in agriculture, biomedicine and environmental studies (Ed.R.W.Li), Nova Science Publishers 61-78.

Statistics Kingdom. 2017. Multiple linear regression calculator. https://www.statskingdom.com/410multi_linear_regression.html

Stevanovic M, Boukéké-Lesplulier T, Hupe L, Hasty J, Bittihn P, Schultz D. 2022. Nutrient gradients mediate complex colony-level antibiotic responses in structured microbial populations. Front Microbiol 13.

Stover CK, Pham XQ, Erwin AL, Mizoguchi SD, Warrener P, Hickey MJ, Brinkman F S, Hufnagle WO, Kowalik DJ, Lagrou M, Garber RL, Goltry L, Tolentino E, Westbrock-Wadman S, Yuan Y, Brody LL, Coulter SN, Folger KR, Kas A, Larbig K, … Olson M V. 2000. Complete genome sequence of *Pseudomonas aeruginosa* PAO1, an opportunistic pathogen. Nature 406:959–964.

Taboada B, Estrada K, Ciria R, Merino E. 2018. Operon-mapper: a web server for precise operon identification in bacterial and archaeal genomes. Bioinformatics 34:4118–4120.

Tamma PD, Heil EL, Justo JA, Mathers AJ, Satlin MJ, Bonomo RA. 2024. Infectious diseases society of America 2024 guidance on the treatment of antimicrobial-resistant gram-negative infections. Clin Infect Dis. ciae403.

Taylor PK, Zhang L, Mah TF. 2019. Loss of the two-component system TctD-TctE in *Pseudomonas aeruginosa* affects biofilm formation and aminoglycoside susceptibility in response to citric acid. mSphere 4:e00102-19.

Thornton CS, Surette MG. 2021 . Potential contributions of anaerobes in Cystic fibrosis airways. J Clin Microbiol 59:e01813-19.

Weiss Nielsen M, Sternberg C, Molin S, Regenberg B. 2011. *Pseudomonas aeruginosa* and *Saccharomyces cerevisiae* biofilm in flow cells. J Vis Exp.

World Health Organization. 2024. WHO bacterial priority pathogens list, 2024: Bacterial pathogens of public health importance to guide research, development and strategies to prevent and control antimicrobial resistance. https://www.who.int/publications/i/item/9789240093461.

Winsor GL, Griffiths EJ, Lo R, Dhillon BK, Shay JA, Brinkman FSL. 2016. Enhanced annotations and features for comparing thousands of *Pseudomonas genomes* in the *Pseudomonas* genome database. Nucleic Acids Res 44:D646–D653.

Winsor GL, Lam DKW, Fleming L, Lo R, Whiteside MD, Yu NY, Hancock REW, Brinkman FSL. 2010. *Pseudomonas* Genome Database: improved comparative analysis and population genomics capability for Pseudomonas genomes. Nucleic Acids Res 39:D596–D600.

Xu M, Fralick D, Zheng JZ, Wang B, Tu XM, Feng C. 2017. The differences and similarities between two-sample t-test and paired t-test. Shanghai Arch Psychiatry 29:184–188

Yoon MY, Lee K-M, Park Y, Yoon SS. 2011. Contribution of cell Elongation to the biofilm formation of *Pseudomonas aeruginosa* during anaerobic respiration. PLoS ONE 6:e16105.

Zhang L, Hinz AJ, Nadeau JP, Mah TF. 2011. *Pseudomonas aeruginosa* tssC1 links type VI secretion and biofilm-specific antibiotic resistance. J Bacteriol 193:5510–5513.

Zhang L, Mah TF. 2008. Involvement of a novel efflux system in biofilm-specific resistance to antibiotics. J Bacteriol 190:4447–4452.